

Preparation and Reactions of Base-Free Bis(1,3-di-*tert*-butylcyclopentadienyl)titanium, Cp'₂Ti, and Related Compounds

Marc D. Walter, Chadwick D. Sofield, and Richard A. Andersen*

Department of Chemistry and Chemical Sciences Division of Lawrence Berkeley National Laboratory, University of California, Berkeley, California 94720

Received December 8, 2007

The titanium(III) metallocene derivatives [1,3-(Me₃C)₂C₅H₃]₂TiX, Cp'₂TiX, X = Cl, Me, H, OH, are prepared and shown to be monomeric with a d¹ electron configuration by solid state magnetic susceptibility studies over the temperature range 5–300 K. Reduction of the chloride by potassium amalgam in an argon atmosphere yields the base-free titanocene Cp'₂Ti, which is a spin triplet over the temperature range 5–300 K. In contrast, reduction in a nitrogen atmosphere gives the dimetal metallocene Cp'₂Ti(N₂)TiCp'₂, which shows a singlet–triplet equilibrium over the temperature range 5–300 K, which can be modeled by Heisenberg coupling with $-2J = 210 \text{ cm}^{-1}$. The base-free titanocene reacts reversibly with H₂ or C₂H₄ to give Cp'₂TiH₂ and Cp'₂Ti(C₂H₄), respectively. Both adducts are characterized by X-ray crystallography. The base-free titanocene reacts irreversibly with PhC≡CPh or N₂O to give Cp'₂Ti(PhC≡CPh) and Cp'₄Ti₂(μ-O), which are characterized by X-ray crystallography. In contrast Cp'₂Ti(C₂H₄) reacts with N₂O to give the bisoxo-bridged dimetal derivative Cp'₄Ti₂(μ-O)₂.

Introduction

The 1,3-(Me₃C)₂C₅H₃ ligand, abbreviated Cp' in this paper, has not been used as extensively as the C₅H₅ (Cp) or the Me₅C₅ (Cp*) ligands in the preparation of metallocene derivatives of the early d-transition metals. We have used it to prepare f-block metallocenes since the [1,3-(Me₃C)₂C₅H₃]₂M fragment is potentially diastereotopic, a property that can be useful in dynamic NMR studies.¹ A possible reason for the lack of interest in the 1,3-(Me₃C)₂C₅H₃ ligand is that the chemical and physical properties of, for example, Cp'₂TiX₂ or Cp'₂TiX are likely to be comparable to those of their Me₅C₅ analogues. Structurally this is true, as shown by the bond distances and angles, when X = Cl, in the first four entries in Table 1. The major difference in the four structures is that the ring(centroid)–Ti–ring(centroid) angle is larger by 5–10° in the Me₅C₅ case, presumably a reflection of the larger steric repulsion in the bent sandwich structure with bulkier cyclopentadienyl ligands, while the TiCl distances within each set are essentially equal. However, the bond dissociation enthalpies (BDEs) of the group 4 metallocene derivatives show that, for example, the Ti–I BDE of Cp'₂TiI is 41 kcal mol⁻¹, whereas that of (C₅Me₅)₂TiI is 52 kcal mol⁻¹.² The weaker Ti–I bond extends to the BDEs of zirconium and hafnium metallocene diiodides and dimethyls, which are about 20 kcal mol⁻¹ weaker for Cp'₂MX₂ relative to those of (C₅Me₅)₂MX₂. While the structural parity but thermochemical disparity is doubtless due to several factors, steric effects are probably the origin of the differences. Assuming that the weakened Ti–I bond carries over to other Ti–X and TiX₂ bonds that are of more interest to organometallic chemists, such as Ti–Me or Ti–H, these titanium derivatives might have rather

different chemistry than do the (C₅Me₅)₂TiX or (C₅Me₅)₂TiX₂ derivatives. It is in this spirit of exploration that the studies described in this paper were initiated.

Results and Discussion

Synthesis, Properties, and Metathesis Reactions of Cp'₂TiCl. The preparation of Cp'₂TiCl has been described previously;^{2,3} our preparation using Cp'₂Mg and TiCl₃(thf)₂ is given in the Experimental Section. Cp'₂TiCl shows a broad resonance at δ 3.82 ppm ($\nu_{1/2} = 430 \text{ Hz}$) in the ¹H NMR spectrum in C₆D₆ at 21 °C. It is monomeric in the solid state, as shown by single-crystal X-ray diffraction (Table 1).³ Oxidation with CCl₄ or HgCl₂ yields the known diamagnetic Cp'₂TiCl₂ (see Experimental Section for details).^{3,4}

Addition of MeLi to Cp'₂TiCl gives Cp'₂TiMe, Scheme 1. The monomethyl derivative is also obtained from the reaction of Cp'₂TiCl₂ and 2 equiv of MeLi in good yield. As noted in the Introduction, the bond dissociation enthalpy (BDE) of Cp'₂TiI is 11 kcal mol⁻¹ less than that of (C₅Me₅)₂TiI, and if the lowered BDE is extrapolated to the Ti–Me bonds, it is not surprising that Cp'₂TiMe₂ is not isolated. The green methyl derivative is obtained by crystallization from hexane; it sublimes at 60–70 °C in diffusion pump vacuum. The ¹H NMR spectrum consists of a broad resonance at 3.61 ppm ($\nu_{1/2} = 430 \text{ Hz}$).

The methyl complex is converted, with degassed water, to blue-purple Cp'₂TiOH, mp 110–112 °C. The EI-mass spectrum shows the molecular ion as the base peak, and the ¹H NMR spectrum consists of a broad resonance at 3.66 ppm ($\nu_{1/2} = 670 \text{ Hz}$). The IR spectrum exhibits a sharp absorption band due to the $\nu_{\text{O-H}}$ stretch at 3668 cm⁻¹, somewhat higher than found in (C₅Me₅)₂TiOH ($\nu_{\text{O-H}} = 3652 \text{ cm}^{-1}$).⁹

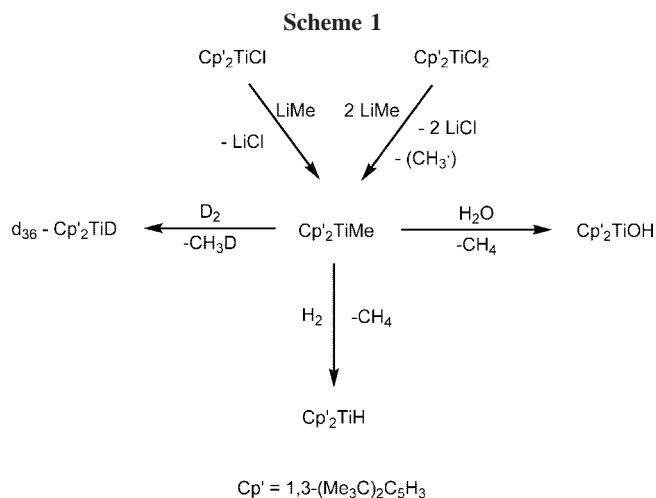
* To whom correspondence should be addressed. E-mail: raandersen@lbl.gov.

(1) Lukens, W. W.; Beshouri, S. M.; Stuart, A. L.; Andersen, R. A. *Organometallics* **1999**, *18*, 1247–1252.

(2) King, W. A.; Di Bella, S.; Gulino, A.; Lanza, G.; Fragala, I. L.; Stern, C. L.; Marks, T. J. *J. Am. Chem. Soc.* **1999**, *121*, 355–366.

(3) Urazowski, I. F.; Ponomaryov, V. I.; Ellert, O. G.; Nifant'ev, I. E.; Lemenovskii, D. A. *J. Organomet. Chem.* **1988**, *356*, 181–193.

(4) Okuda, J. *J. Organomet. Chem.* **1990**, *385*, C39–C42.



In order to examine the acidity of the OH proton, its reactivity toward $\text{Cp}'_2\text{TiMe}$ and D_2 was investigated. It reacts with $\text{Cp}'_2\text{TiMe}$ slowly at 65°C to form CH_4 , HCp' , and a new unidentified Ti(III)-containing compound in small yield, which decomposes on further heating. The hydroxide decomposes immediately in the presence of D_2 (1 atm) to yield HCp' and unidentified organic compounds. No deuterium incorporation into the Cp' ring is found, as judged by the ^2H NMR spectrum, and the role of D_2 in the reaction is unclear.

The reaction of $\text{Cp}'_2\text{TiMe}$ with H_2 is different from that with water. Thus, a red solution is formed immediately after exposing a green pentane solution of $\text{Cp}'_2\text{TiMe}$ to 1 atm of H_2 , from which $\text{Cp}'_2\text{TiH}$ may be crystallized at -80°C as brick-red blocks, mp $147\text{--}149^\circ\text{C}$. The ^1H NMR spectrum consists of a broad resonance at 2.68 ppm ($\nu_{1/2} = 140$ Hz). Although the hydride resonance cannot be located in the ^1H NMR spectrum, a strong TiH absorption ($\nu_{\text{Ti-H}}$) at 1550 cm^{-1} is observed in the IR spectrum, which shifts to 1120 cm^{-1} when D_2 is used in the synthesis. This is in good agreement with the expected H/D isotopic shift [$\nu_{\text{Ti-H}}/\nu_{\text{Ti-D}} = 1.38$]. The monomeric hydrides $(\text{C}_5\text{Me}_5)_2\text{TiH}$ and $(\text{C}_5\text{Me}_4\text{Ph})_2\text{TiH}$ have $\nu_{\text{Ti-H}}$ at 1490 and 1505 cm^{-1} , respectively.^{10,11} Exposure to 1 atm of D_2 at room temperature not only yields the deuteride $\text{Cp}'_2\text{TiD}$, but H/D scrambling into the CMe_3 groups of the Cp' ring occurs, which is also observed for $(\text{C}_5\text{Me}_5)_2\text{TiH}$ and $(\text{C}_5\text{Me}_4\text{Ph})_2\text{TiH}$.^{10,11}

Upon exposure to high pressure of deuterium (9 atm) for 6 days, nearly complete deuterium incorporation into the CMe_3 groups is achieved, as shown by the composition of the molecular ion of $\text{Cp}'\text{D}$ formed on hydrolysis with H_2O (Figure 1). This result is confirmed by ^2H NMR spectroscopy, since $d_{36}\text{-Cp}'_2\text{TiD}$ exhibits a sharp resonance at 2.69 ppm ($\nu_{1/2} = 6$ Hz) in the ^2H NMR spectrum due to the CMe_3 groups. No H/D scrambling into the methine positions is observed, which is consistent with the GC-MS results. The ^2H NMR resonance is expected to be narrower than the corresponding ^1H NMR

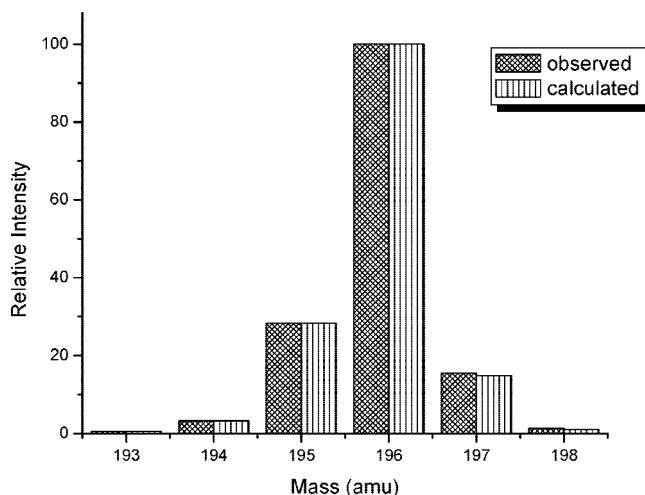


Figure 1. Deuterium incorporation into the Cp' ring in $\text{Cp}'_2\text{TiD}$ (9 atm, 6 days, atmosphere exchanged once). The ring deuterated deuteride was crystallized from pentane at -65°C and hydrolyzed with H_2O , and the hydrolysate was analyzed by GC-MS. The simulation is based on the following isotopic distribution: $\text{C}_{13}\text{D}_{15}\text{H}_7$ 0.5%, $\text{C}_{13}\text{D}_{16}\text{H}_6$ 2.5%, $\text{C}_{13}\text{D}_{17}\text{H}_5$ 21.8%, and $\text{C}_{13}\text{D}_{18}\text{H}_4$ 75.2%.

resonance by a factor of $\gamma_{\text{H}}^2/\gamma_{\text{D}}^2 = 42.5$ based on the Solomon–Bloembergen equation.^{12,13} The observed ratio of 23.3 in this case is less than the theoretical value; however this is not unexpected, as most metal complexes exhibit smaller ratios; for example, in $\text{Ti}(\text{acac})_3$ the ratio is on the order of 30.¹⁴ A resonance for Ti–D is not observed.

Deuterium incorporation into CMe_3 groups has been observed previously in the case of $[1,2,4\text{-(Me}_3\text{C)}_3\text{C}_5\text{H}_2]_2\text{CeH}$.^{15,16} A mechanism that accounts for deuterium incorporation is likely to be similar; that is, the initially formed deuteride eliminates HD from a methyl hydrogen of the CMe_3 group, forming a metallacycle. The metallacycle then reacts with additional D_2 to re-form the deuteride with incorporation of deuterium into the Cp' ligand. The latter two steps proceed until deuterium has been completely exchanged in the CMe_3 groups. These steps constitute an equilibrium process wherein D_2 replaces HD due to the much higher concentration of D_2 in the reaction mixture.

Another remarkable property of $\text{Cp}'_2\text{TiH}$ is its thermochromic behavior. When a pentane solution of $\text{Cp}'_2\text{TiH}$ under 1 atm of N_2 is cooled to -80°C , it changes color from red to deep blue. From EPR studies on $(\text{C}_5\text{Me}_4\text{Ph})_2\text{TiH}$, it is known that titanium hydride complexes can form nitrogen adducts, such as $(\text{C}_5\text{Me}_4\text{Ph})_2\text{Ti}(\text{H})(\text{N}_2)$,¹¹ and therefore the color change might be due to N_2 complex formation. Subsequently, a pentane solution of $\text{Cp}'_2\text{TiH}$ was exposed to 18 atm pressure of N_2 and alternatively to a mixture of 8 atm of N_2 and 7 atm of H_2 ; however no reaction was observed. $\text{Cp}'_2\text{TiH}$ does not react with C_6F_6 , $\text{C}_6\text{F}_5\text{H}$, or $\text{C}_6\text{F}_4\text{H}_2$ in C_6D_6 at room temperature or elevated temperatures (65°C). But on exposure to 1 atm of CO , a new Ti(III)-containing compound is initially formed, which decomposes over time. After 6 h at 65°C only resonances due to HCp' and $\text{Cp}'_2\text{Ti}(\text{CO})_2$ can be identified; the carbonyl derivative is described below.

(5) McKenzie, T. C.; Sanner, R. D.; Bercaw, J. E. *J. Organomet. Chem.* **1975**, *102*, 457–466.

(6) Pattiasina, J. W.; Heeres, H. J.; van Bulhuis, F.; Meetsma, A.; Teuben, J. H.; Spek, A. L. *Organometallics* **1987**, *6*, 1004–1010.

(7) Auburn, P. R.; Bercaw, J. E. *J. Am. Chem. Soc.* **1983**, *105*, 1136–1143.

(8) Horacek, M.; Kupfer, V.; Thewalt, U.; Stepnicka, P.; Polasek, M.; Mach, K. *Organometallics* **1999**, *18*, 3572–3578.

(9) Horacek, M.; Gyepes, R.; Kubista, J.; Mach, K. *Inorg. Chem. Commun.* **2004**, *7*, 155–159.

(10) Lukens, W. W.; Matsunaga, P. T.; Andersen, R. A. *Organometallics* **1998**, *17*, 5240.

(11) de Wolf, J. M.; Meetsma, A.; Teuben, J. H. *Organometallics* **1995**, *14*, 5466–5468.

(12) Bloembergen, N. *J. Chem. Phys.* **1957**, *27*, 572–573.

(13) Solomon, I. *Phys. Rev.* **1955**, *99*, 559–565.

(14) La Mar, G. N.; Horrocks, W. D.; Holm, R. H. *NMR of Paramagnetic Molecules*; Academic Press: New York, 1973; pp 287–289; 638–640.

(15) Maron, L.; Werkema, E. L.; Perrin, L.; Eisenstein, O.; Andersen, R. A. *J. Am. Chem. Soc.* **2005**, *127*, 279–292.

(16) Werkema, E. L.; Messines, E.; Perrin, L.; Maron, L.; Eisenstein, O.; Andersen, R. A. *J. Am. Chem. Soc.* **2005**, *127*, 7781–7795.

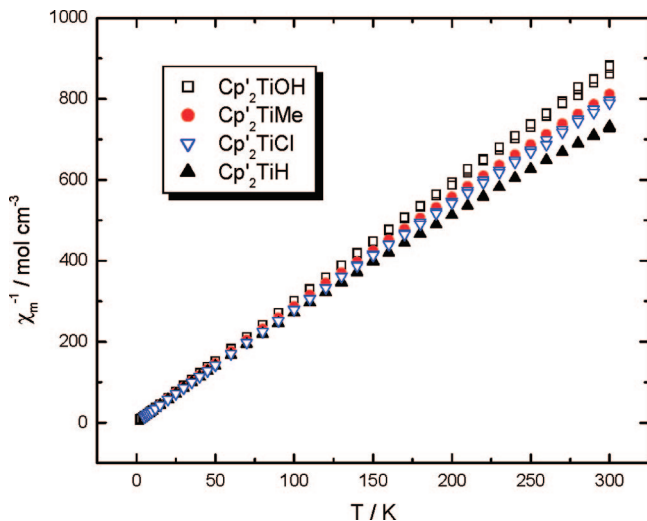


Figure 2. χ_m^{-1} vs T plot for $\text{Cp}'_2\text{TiX}$ ($X = \text{H, Me, OH, and H}$).

Interestingly, the surface of $\text{Cp}'_2\text{TiH}$ changes color from red to blue on prolonged exposure to a N_2 atmosphere in the solid state. When this blue material is dissolved in C_6D_6 , a red solution is obtained and no differences are noted in the ^1H NMR spectra relative to a sample of freshly prepared $\text{Cp}'_2\text{TiH}$. Furthermore, the IR spectrum recorded as a Nujol mull is identical to that of the red material. The stability of $\text{Cp}'_2\text{TiH}$ toward N_2 is quite remarkable, compared to $[\text{1,3}-(\text{Me}_3\text{Si})_2\text{C}_5\text{H}_3]_2\text{TiH}$, abbreviated as $\text{Cp}''_2\text{TiH}$, which in the presence of nitrogen reacts immediately in C_6D_6 solution to form the known dinitrogen complex $(\text{Cp}''_2\text{Ti})_2(\text{N}_2)$, as identified by its IR and ^1H NMR spectrum.¹⁷

Solid State Magnetism (SQUID) of $\text{Cp}'_2\text{TiX}$. Solid state magnetism is a useful tool to distinguish between monomeric and dimeric Ti(III) complexes. Monomeric $\text{Cp}'_2\text{TiX}$ compounds have one unpaired electron in an a_1 orbital (in C_{2v} molecular symmetry),¹⁸ and the magnetic susceptibility obeys Curie law; that is, the χ_m^{-1} vs T plot is linear and the magnetic moment is temperature independent and close to the spin-only value for a $S = 1/2$ system with $\mu_{\text{eff}} = 1.73 \mu_B$. However, in dimeric $[\text{Cp}'_2\text{TiX}]_2$ complexes coupling between the spin centers is observed; that is, the χ_m^{-1} vs T plot is not linear.^{19–21} The χ_m^{-1} vs T plots for a series of monomeric $\text{Cp}'_2\text{TiX}$ ($X = \text{H, Me, OH, Cl}$) are shown in Figure 2. They are linear from 5 to 300 K with $\mu_{\text{eff}} \approx 1.7 \mu_B$, consistent with the expected $S = 1/2$ ground state (Table 2). The individual χ_m^{-1} vs T and μ_{eff} vs T plots are provided in the Supporting Information.

Synthesis and Properties of $\text{Cp}'_2\text{Ti}$. The reduction of $\text{Cp}'_2\text{TiCl}$ with various reducing agents was explored; the most successful one was potassium amalgam in hexane under argon. Blue crystals of $\text{Cp}'_2\text{Ti}$ were obtained from the mother liquor, mp 148–149 °C. The titanocene sublimes at 60–70 °C under diffusion pump vacuum, and it gives a molecular ion in the mass spectrum. Due to the flat-plate-like morphology of the

titanocene crystals, and in spite of several attempts, no suitable crystals for an X-ray diffraction experiment were obtained.²²

A very broad resonance is observed in the ^1H NMR spectrum in C_6D_6 (30 °C) at 3.2 ppm ($\nu_{1/2} = 300$ Hz), presumably due to the CMe_3 groups, indicative of a paramagnetic compound; the methine ring resonances are not observed. ^1H NMR spectroscopy is only moderately useful in these systems due to extreme line broadening and a relatively limited chemical shift range differentiating the Ti(II) and Ti(III) species (Table 2). A more convenient way to detect $\text{Cp}'_2\text{TiCl}$ contamination, due to incomplete reduction, is EPR and UV–vis spectroscopy, as these physical methods are very sensitive to small amounts of impurities. For this reason, EPR spectra of $\text{Cp}'_2\text{Ti}$ and $\text{Cp}'_2\text{TiCl}$ solutions are recorded in toluene solution at room temperature. However, $\text{Cp}'_2\text{Ti}$ does not give an EPR spectrum in toluene solution at room temperature; $(\text{C}_5\text{Me}_4\text{SiMe}_3)_2\text{Ti}$ is also EPR silent.⁸ On the other hand, $\text{Cp}'_2\text{TiCl}$ gives a strong resonance at $g_{\text{av}} = 1.9677$. The room-temperature UV–vis spectra consist of broad absorptions in both of these metallocenes. $\text{Cp}'_2\text{Ti}$ has its absorption at 589 nm ($\epsilon = 121 \text{ L mol cm}^{-1}$) probably due to the spin-allowed $e_{2g}^2 \rightarrow e_{2g}^1 e_{2g}^1$ transition, while $\text{Cp}'_2\text{TiCl}$ exhibits two absorptions at 625 nm ($\epsilon = 96 \text{ L mol cm}^{-1}$) and 560 nm ($\epsilon = 107 \text{ L mol cm}^{-1}$), which are assigned to $1a_1 \rightarrow 2a_1$ and $1a_1 \rightarrow b_1$ transitions as in $(\text{C}_5\text{Me}_5)_2\text{TiCl}$ (Figure 3).²³

In the solid state, a plot of χ_m^{-1} vs T for $\text{Cp}'_2\text{Ti}$ is linear from 5 to 300 K with $\mu_{\text{eff}} = 2.44 \mu_B$ (Figure 4).²⁴ This value is close to the solid state magnetic moment for $(\text{C}_5\text{Me}_5)_2\text{Ti}$ of $2.6 \mu_B$ ²⁵ and the room-temperature solution moment of $2.4 \mu_B$ for $(\text{C}_5\text{Me}_4\text{SiMe}_2\text{CMe}_3)_2\text{Ti}$.²⁶ The magnetic moment of $2.44 \mu_B$ for $\text{Cp}'_2\text{Ti}$ implies that the titanocene has a triplet ground state with an electronic configuration of either e_{2g}^2 or $e_{2g}^1 a_{1g}^1$ (D_{5d} symmetry).^{27,28}

Reactions of $\text{Cp}'_2\text{Ti}$. 1. Dinitrogen. If the reduction of $\text{Cp}'_2\text{TiCl}$ is performed under an atmosphere of N_2 , a 2:1 dinitrogen adduct $(\text{Cp}'_2\text{Ti})_2(\text{N}_2)$ can be isolated by crystallization from pentane as deep blue crystals with a metallic luster. The same product is obtained on exposure of $\text{Cp}'_2\text{Ti}$ to N_2 . During this process the color changes from a “dull” blue to deep blue; even in the solid state the surface of the crystals perceptively darken when exposed to even trace amounts of N_2 . As a powder, the darkening of the surface is rapid. This and related reactions of $\text{Cp}'_2\text{Ti}$ are shown in Scheme 2.

(22) We encountered similar problems with $\text{Cp}'_2\text{V}$. However, crystals of $\text{Cp}'_2\text{Cr}$ gave an excellent data set and a good X-ray structure. The $\text{Cp}'_2\text{Cr}$ and $\text{Cp}'_2\text{Fe}$ crystallize in an orthorhombic crystal lattice, whereas $\text{Cp}'_2\text{Ti}$ and $\text{Cp}'_2\text{V}$ crystallize in a tetragonal lattice: $\text{Cp}'_2\text{Ti}$: $a = 12.0614(11) \text{ \AA}$, $b = 12.0614(11) \text{ \AA}$, $c = 8.5317(11) \text{ \AA}$, $\alpha = \beta = \gamma = 90^\circ$; $\text{Cp}'_2\text{V}$: $a = 11.9810(11) \text{ \AA}$, $b = 11.9810(11) \text{ \AA}$, $c = 8.6312(11) \text{ \AA}$, $\alpha = \beta = \gamma = 90^\circ$; $\text{Cp}'_2\text{Cr}$: $a = 11.7750(6) \text{ \AA}$, $b = 12.4122(6) \text{ \AA}$, $c = 32.6410(20) \text{ \AA}$, $\alpha = \beta = \gamma = 90^\circ$, *Pccn*: Schultz, M. *Acta Crystallogr.* **2007**, *E63*, m3085. $\text{Cp}'_2\text{Fe}$: $a = 11.561(2) \text{ \AA}$, $b = 12.113(2) \text{ \AA}$, $c = 33.437(6) \text{ \AA}$, $\alpha = \beta = \gamma = 90^\circ$, *Pccn*: Boese, R.; Blaeser, D.; Kuhn, N. *Z. Kristallogr.* **1993**, *205*, 282–284.

(23) Lukens, W. W.; Smith, M. R.; Andersen, R. A. *J. Am. Chem. Soc.* **1996**, *118*, 1719–1728.

(24) The moment might be low due to the extreme sensitivity of the base-free titanocene to trace amounts of N_2 in argon even in the solid state. This is particularly true for those samples that are finely ground, i.e., those used for the magnetic susceptibility measurements.

(25) Bercaw, J. E. *J. Am. Chem. Soc.* **1974**, *96*, 5087–5095. The value of μ_{eff} varies from $2.60 \mu_B$ at 298 K to $2.48 \mu_B$ at 129 K. In footnote 32 of ref 29, an effective magnetic moment of $2.15 \mu_B$ is determined in the solid state.

(26) Hitchcock, P. B.; Kerton, F. M.; Lawless, G. A. *J. Am. Chem. Soc.* **1998**, *120*, 10264–10265.

(27) Warren, K. D. *Struct. Bonding (Berlin)* **1976**, *27*, 45–159.

(28) Lever, A. B. P., *Inorganic Electronic Spectroscopy*; Elsevier: Amsterdam, 1984; Chapter 7.

(17) Hanna, T. E.; Keresztes, I.; Lobkovsky, E.; Bernskoetter, W. H.; Chirik, P. J. *Organometallics* **2004**, *23*, 3448–3458.

(18) Lauher, J. W.; Hoffmann, R. *J. Am. Chem. Soc.* **1976**, *98*, 1729–1742.

(19) Fieslmann, B. F.; Stucky, G. D. *Inorg. Chem.* **1978**, *17*, 2074–2077.

(20) Jungst, R.; Sekutowski, D.; Davis, J.; Luly, M.; Stucky, G. D. *Inorg. Chem.* **1977**, *16*, 1645–1655.

(21) Francesconi, L. C.; Corbin, D. R.; Hendrickson, D. N.; Stucky, G. D. *Inorg. Chem.* **1979**, *18*, 3074–3080.

Table 1. Selected Bond Distances (Å) and Angles (deg) for Various Titanocene Complexes, Cp' = 1,3-(Me₃C)₂C₅H₃, Described in this Paper

| compound | Ti–C(av) (Å) | Ti–Cp(cent) (Å) | Cp(cent)–Ti–Cp(cent) (deg) | Ti–X (Å) | other (Å) |
|--|--------------|-----------------|----------------------------|----------|---------------|
| (C ₅ Me ₅) ₂ TiCl ₂ ^a | 2.44(2) | 2.13 | 137 | 2.349(2) | |
| Cp' ₂ TiCl ₂ ^b | 2.44(2) | 2.12 | 132 | 2.349(1) | |
| (C ₅ Me ₅) ₂ TiCl ^c | 2.39(1) | 2.06 | 144 | 2.363(1) | |
| Cp' ₂ TiCl ^b | 2.39(2) | 2.07 | 135 | 2.337(1) | |
| Cp' ₂ Ti(PhC≡CPh) ^d | 2.44(3) | 2.12 | 134 | 2.079(2) | C≡C, 1.300(6) |
| Cp' ₂ Ti(C ₂ H ₄) ^d | 2.42(6) | 2.09 | 138 | 2.169(6) | C=C, 1.427(5) |
| (C ₅ Me ₅) ₂ Ti(C ₂ H ₄) ^e | 2.41(4) | 2.09 | 144 | 2.160(4) | C=C, 1.438(5) |
| (C ₅ Me ₄ SiMe ₃) ₂ Ti(C ₂ H ₄) ^f | 2.45(5) | 2.13 | 147 | 2.167(4) | C=C, 1.442(9) |
| Cp' ₂ TiH ₂ ^d | 2.37(1) | 2.04 | 145 | 1.60(2) | |

^a Ref 5. ^b Ref 3; there are several errors in Table 3 of this reference, the most serious of which is the Ti–C(av) distance in Cp'₂TiCl₂ is 2.435 ± 0.019 Å, not 2.449 Å, and the Cp(cent)–Ti–Cp(cent) angle in Cp'₂TiCl₂ is 132°, not 121°. ^c Ref 6. ^d This work. ^e Ref 7. ^f Ref 8.

Table 2. Some Physical Properties of Cp'₂Ti- and Cp''₂Ti-Containing Compounds, Cp' = 1,3-(Me₃C)₂C₅H₃ and Cp'' = 1,3-(Me₃Si)₂C₅H₃

| compound | color | mp [°C] | ¹ H NMR ^a | μ _{eff} (300 K) [μ _B] ^c |
|---|--------------|----------------|--|---|
| Cp' ₂ TiCl | blue | 145–146 | 3.82 (430) | 1.74 |
| Cp' ₂ TiMe | green | 128–129 | 3.61 (430) | 1.72 |
| Cp' ₂ TiOH | blue-purple | 110–112 | 3.66 (670) | 1.66 |
| Cp' ₂ TiH | red | 147–149 | 2.68 (140) | 1.81 |
| Cp' ₂ Ti | blue | 148–149 | 3.2 (300) ^b | 2.44 |
| (Cp' ₂ Ti) ₂ (N ₂) | deep blue | 130–140 (dec.) | 3.60 (60) | 1.46 ^d |
| Cp'' ₂ TiCl | blue | 153–154 | 2.66 (340) | 1.73 |
| (Cp'' ₂ Ti) ₂ (N ₂) | deep blue | 143–144 (dec.) | 2.65 (170) | 1.44 ^d |
| Cp' ₂ TiCl ₂ | red | 223–225 | 1.29 (s, 36H, CMe ₃) 5.81 (d, 4H, ⁴ J _{CH} = 3 Hz, ring-CH) 6.77 (t, 2H, ⁴ J _{CH} = 3 Hz, ring-CH) | diamagnetic |
| Cp' ₂ Ti(C ₂ H ₄) | yellow-green | 122–123 | 1.06 (s, 36H, CMe ₃) 2.94 (s, 4H, C ₂ H ₄) 4.34 (d, 4H, ⁴ J _{CH} = 2.4 Hz, ring-CH) 9.26 (t, 2H, ⁴ J _{CH} = 2.4 Hz, ring-CH) | diamagnetic |
| Cp' ₂ Ti(CO) ₂ | red | 125–127 | 1.17 (s, 36H, CMe ₃) 4.83 (d, 4H, ⁴ J _{CH} = 2 Hz, ring-CH) 5.13 (t, 2H, ⁴ J _{CH} = 2 Hz, ring-CH) | diamagnetic |
| Cp' ₂ Ti(PhCCPh) | red-orange | 169–170 | 1.12 (s, 36H, CMe ₃) 5.51 (d, 4H, ⁴ J _{CH} = 2.6 Hz, ring-CH) 7.99 (t, 2H, ⁴ J _{CH} = 2.6 Hz, ring-CH) 6.89–7.11 (C ₆ H ₅ resonances, overlapping 10H) | diamagnetic |
| Cp' ₂ TiH ₂ | red | 152–154 (dec) | 1.13 (s, 36H, CMe ₃) ^e 2.62 (s, 2H, Ti–H) ^e 5.10 (d, 4H, ⁴ J _{CH} = 3 Hz, ring-CH) ^e 8.01 (t, 2H, ⁴ J _{CH} = 3 Hz, ring-CH) ^e | diamagnetic |
| (Cp' ₂ TiO) ₂ | red | 228–229 | 1.36 (s, 18H, CMe ₃) 1.45 (s, 18H, CMe ₃) 5.78 (d, 2H, ⁴ J _{CH} = 1.3 Hz, ring-CH) 6.04 (d, 2H, ⁴ J _{CH} = 2.7 Hz, ring-CH) 6.33 (t, 1H, ⁴ J _{CH} = 1.3 Hz, ring-CH) 6.53 (t, 1H, ⁴ J _{CH} = 2.7 Hz, ring-CH) | diamagnetic |

^a Recorded in C₆D₆ at 21 °C, unless specified otherwise. The line width at half-peak height (Hz) for paramagnetic compounds is given in parentheses.

^b Recorded in C₆D₆ at 30 °C. ^c The magnetic moment is given per titanium center and calculated from the value of χT at 300 K using the relation μ_{eff} = 2.828(χT)^{0.5}. ^d Strongly antiferromagnetically coupled Ti(III) centers. ^e Recorded in C₇D₈ at –54 °C.

The structure of the N₂ complex is presumably related to those of the C₅Me₅, 1,3-(Me₃Si)₂C₅H₃, Me₄C₅H, and Me₄C₅R (R = iPr, tBu) analogues.^{17,29–31} It is noteworthy that (C₅Me₄SiMe₃)₂Ti⁸ and (C₅Me₄SiMe₂CMe₃)₂Ti²⁶ ignore dinitrogen at 1 atm pressure at room temperature, but at low temperatures the base-free titanocenes (C₅Me₄R)₂Ti (R = SiMe₃, SiMe₂Ph, CMe₃, and CHMe₂) reversibly bind N₂ to form the 1:1 and 1:2 adducts (C₅Me₄R)₂Ti(N₂) and (C₅Me₄R)₂Ti(N₂)₂, respectively.^{32,33}

The dinitrogen adduct, (Cp'₂Ti)₂(N₂), loses N₂ when heated in a sealed tube between 130 and 140 °C, as bubbles are

observed when the material melts, and in the inlet of the mass spectrometer since the molecular ion is identical to that of the base-free titanocene. Sublimation at 60–70 °C in a dynamic diffusion pump vacuum also yields the base-free titanocene. The UV–vis spectrum of (Cp'₂Ti)₂(N₂) shows a very intense and broad feature at 603 nm (ε = 1850 L mol cm^{–1}) (Figure 3 and Table 3).

The solid state magnetic susceptibility of the dinitrogen adduct is of considerable interest relative to electron exchange behavior. The 1/χ vs T and χ vs T plots are indicative of strong antiferromagnetic coupling between the spin carriers, and the corrected effective magnetic moment at room temperature is 2.07 μ_B per dimer (Figure 5). The magnetic data can be simulated, assuming that two d¹-spin carriers are coupled across a (N₂)^{2–} bridge (Figure 6), using the Bleaney–Bowers equation (eq 1).^{34,35} The singlet–triplet separation is equal to –2J, Nα represents the temperature-independent paramagnetism (TIP),

(29) Sanner, R. D.; Duggan, D. M.; McKenzie, T. C.; Marsh, R. E.; Bercaw, J. E. *J. Am. Chem. Soc.* **1976**, *98*, 8358–8365.

(30) de Wolf, J. J.; Blaauw, R.; Meetsma, A.; Teuben, J. H.; Gyepes, R.; Varga, V.; Mach, K.; Veldman, N.; Spek, A. L. *Organometallics* **1996**, *15*, 4977–4983.

(31) Hanna, T. E.; Bernskoetter, W. H.; Bouwkamp, M. W.; Lobkovsky, E.; Chirik, P. J. *Organometallics* **2007**, *26*, 2431–2438.

(32) Hanna, T. E.; Lobkovsky, E.; Chirik, P. J. *J. Am. Chem. Soc.* **2004**, *126*, 14688–14689.

(33) Hanna, T. E.; Lobkovsky, E.; Chirik, P. J. *J. Am. Chem. Soc.* **2006**, *128*, 6018–6019.

(34) Kahn, O., *Molecular Magnetism*; VCH: New York, 1993; pp 131–132.

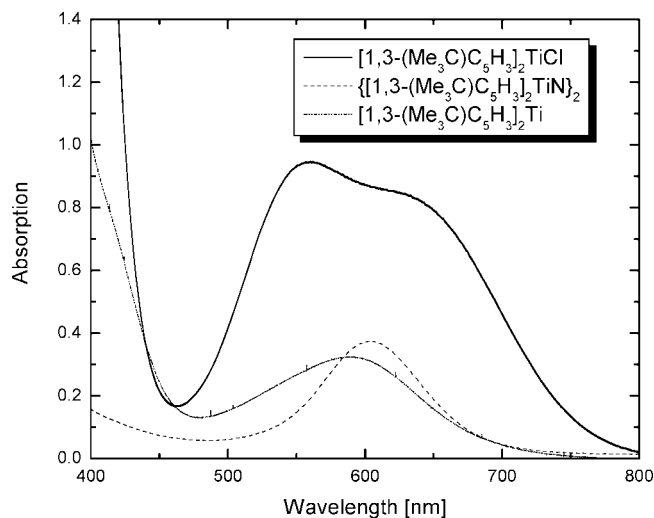


Figure 3. UV-vis spectra of $\text{Cp}'_2\text{TiCl}$, $\text{Cp}'_2\text{Ti}$, and $(\text{Cp}'_2\text{Ti})_2(\text{N}_2)$ in methylcyclohexane.

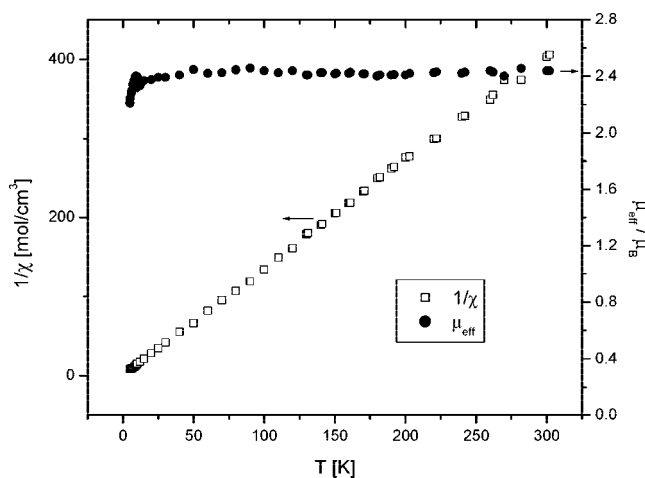
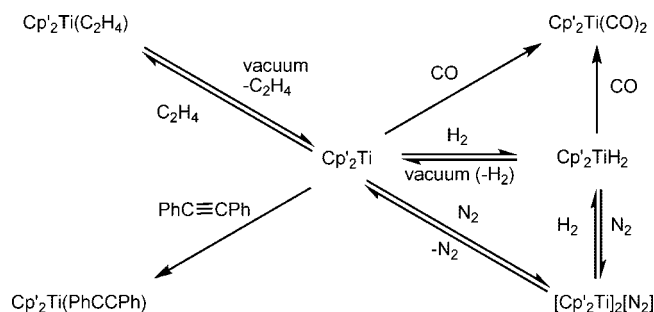


Figure 4. χ_m^{-1} vs T and μ_{eff} vs T plot for $\text{Cp}'_2\text{Ti}$.

Scheme 2



$\text{Cp}' = 1,3\text{-(Me}_3\text{C)}_2\text{C}_5\text{H}_3$

x_p represents the amount of monomeric Ti(III) impurity and with an assumed Curie constant, C , and the g value is determined in a room-temperature solution EPR experiment.

$$\chi_m = \frac{2Ng^2\mu_B^2}{kT} \left[\frac{2e^{2J/kT}}{1 + 3e^{2J/kT}} \right] (1 - x_p) + \left(\frac{C}{T} \right) x_p + N\alpha \quad (1)$$

In this formalism, an equilibrium distribution between the populations in the singlet and triplet state is described by

(35) O'Connor, C. J., *Magnetochemistry-Advances in Theory and Experimentation*. In *Progress in Inorganic Chemistry*; Lippard, S. J., Ed.; J. Wiley & Sons: New York, 1982; Vol. 29, pp 203–285.

Boltzmann statistics. The negative sign of $2J$ means that the spins are antiferromagnetically coupled and the spin singlet is lower in energy than the spin triplet.

The large value of $-2J$ of 210 cm^{-1} is in contrast to the magnetic studies on $[(\text{C}_5\text{Me}_5)_2\text{Ti}]_2(\text{N}_2)$, in which very little exchange coupling was observed, and the effective magnetic moment of $3.08 \mu_B$ per dimer, or $2.18 \mu_B$ per Ti, is temperature invariant from 260 K to ca. 20 K. The value per Ti is intermediate between $1.73 \mu_B$ (spin-only value for Ti(III)) and $2.87 \mu_B$ (spin-only value for Ti(II)). The absence of a signal in the EPR spectrum was interpreted to be in agreement with a linear Ti(II)NNTi(II) geometry, but the large negative orbital

Table 3. Optical Spectra of Some Titanocene Complexes

| compound | λ_{max} in nm ^a |
|--|---|
| $[1,3\text{-(Me}_3\text{C)}_2\text{C}_5\text{H}_3]_2\text{Ti}$ | 589 (121) |
| $[1,3\text{-(Me}_3\text{C)}_2\text{C}_5\text{H}_3]_2\text{TiCl}$ | 625 (96), 560 (107) |
| $\{[1,3\text{-(Me}_3\text{C)}_2\text{C}_5\text{H}_3]_2\text{TiN}\}_2$ | 603 (1850) |
| $[1,3\text{-(Me}_3\text{Si)}_2\text{C}_5\text{H}_3]_2\text{TiCl}$ | 617 (72), 550 (97) |
| $\{[1,3\text{-(Me}_3\text{Si)}_2\text{C}_5\text{H}_3]_2\text{TiN}\}_2$ | 614 (2500) |

^a λ_{max} in nm in methylcyclohexane. Molar extinction coefficient is given in parentheses in units of $\text{L mol}^{-1} \text{ cm}^{-1}$.

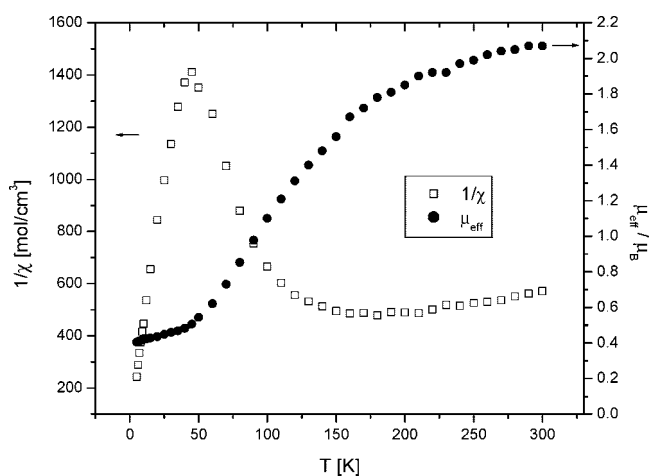


Figure 5. χ_m^{-1} vs T and μ_{eff} (per dimer) vs T plot for $(\text{Cp}'_2\text{Ti})_2(\text{N}_2)$.

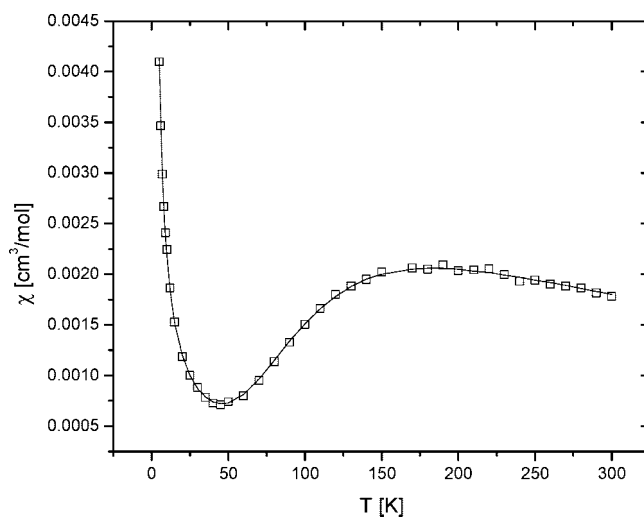


Figure 6. χ vs T plot for $(\text{Cp}'_2\text{Ti})_2(\text{N}_2)$. The g value was fixed as the value obtained from the EPR study ($g_{\text{av}} = 1.9785$); the Curie constant C was set to 0.3436 as determined from the χ vs $1/T$ plot of $\text{Cp}'_2\text{TiCl}$. The parameters were obtained from a least-squares refinement: $J/k = -152 \text{ K}$ (-105 cm^{-1}), $x_p = 5.6\%$, TIP $2.17 \times 10^{-4} \text{ cm}^3/\text{mol}$, and $-2J = 304 \text{ K}$ (210 cm^{-1}).

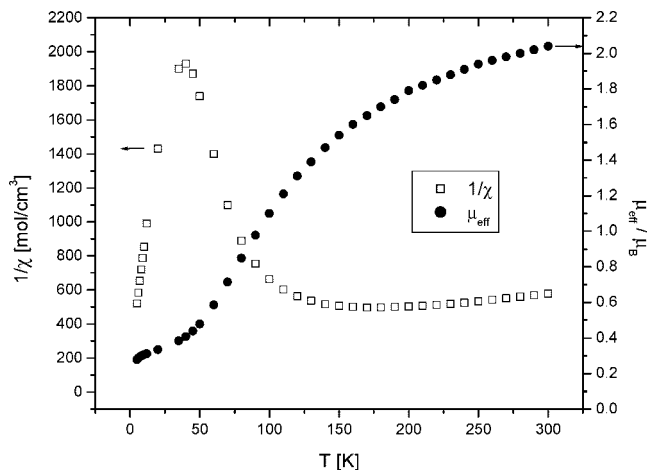


Figure 7. χ_m^{-1} vs T and μ_{eff} (per dimer) vs T plot for $(\text{Cp}''_2\text{Ti})_2(\text{N}_2)$.

contribution reducing the effective magnetic moment was unexplained.²⁹

The difference in the magnetic coupling between the titanium centers in these two metallocene derivatives can be traced to the orientation of the titanocene units relative to each other. A recent theoretical calculation shows that the sign of the coupling constant in the case of $(\text{Cp}_2\text{Ti})_2(\mu\text{-O})$ changes with the relative orientation of the titanocene units.³⁶ In $[(\text{C}_5\text{Me}_5)_2\text{Ti}]_2(\text{N}_2)$ the two titanocene fragments are twisted by 90° with respect to each other, and the molecule has D_{2d} symmetry, treating the C_5Me_5 rings as points.²⁹ Recently, Chirik reported the synthesis and the solid state structure of $\{[(\text{Me}_3\text{Si})_2\text{C}_5\text{H}_3]_2\text{Ti}\}_2(\text{N}_2)$, abbreviated as $(\text{Cp}''_2\text{Ti})_2(\text{N}_2)$.¹⁷ This complex is centrosymmetric, the inversion center is located in the middle of the N–N bond, and the idealized symmetry is D_{2h} . A comparison between the solid state magnetism of the structurally characterized $(\text{Cp}''_2\text{Ti})_2(\text{N}_2)$ and $(\text{Cp}'_2\text{Ti})_2(\text{N}_2)$ provides a test case of the hypothesis that antiferromagnetic interactions between the spin centers is due to the orientation of the titanocene fragments as suggested above. $\text{Cp}''_2\text{TiCl}$ is readily prepared from $\text{TiCl}_3(\text{thf})_3$ and $\text{Cp}''_2\text{Mg}$ (see Experimental Section for details), and the solid state magnetism is provided as Supporting Information. The reduction of $\text{Cp}''_2\text{TiCl}$ with potassium amalgam in boiling toluene under dinitrogen yields the known complex $(\text{Cp}''_2\text{Ti})_2(\text{N}_2)$.¹⁷ The UV–vis spectrum displays a very intense absorption at 614 nm ($\epsilon = 2500 \text{ L mol}^{-1} \text{ cm}^{-1}$) (see Supporting Information for details), and the EPR spectrum at room temperature shows a resonance at $g_{\text{av}} = 1.9777$.

The magnetism of $(\text{Cp}''_2\text{Ti})_2(\text{N}_2)$ closely resembles that of $(\text{Cp}'_2\text{Ti})_2(\text{N}_2)$ not only in the shape of the curve but also in the singlet–triplet splitting, $-2J$, providing evidence that the molecular symmetry of these two complexes is the same, compare Figures 5 and 6 with those of Figures 7 and 8. Qualitatively, the antiferromagnetic coupling as observed in $(\text{Cp}''_2\text{Ti})_2(\text{N}_2)$ and $(\text{Cp}'_2\text{Ti})_2(\text{N}_2)$ can be explained by a simplified molecular orbital model. For a molecule in D_{2h} symmetry such as $(\text{Cp}'_2\text{Ti})_2(\text{N}_2)$ and presumably $(\text{Cp}''_2\text{Ti})_2(\text{N}_2)$, the filled orbitals of N_2 , $(a_{1g})^2$ $(a_{1u})^2$ $(b_{3u})^2$ $(b_{2u})^2$ $(a_{1g})^2$, in D_{2h} symmetry combine with the corresponding $\text{Cp}'_2\text{Ti}$ fragment orbitals.¹⁸ Only the $(a_{1g})^2$ (corresponding to the $2\sigma_g$ orbital (lone pair) in $D_{\infty h}$ symmetry labels) has sufficient energy to combine with the metallocene fragment orbitals, generating three orbitals (using two orbitals

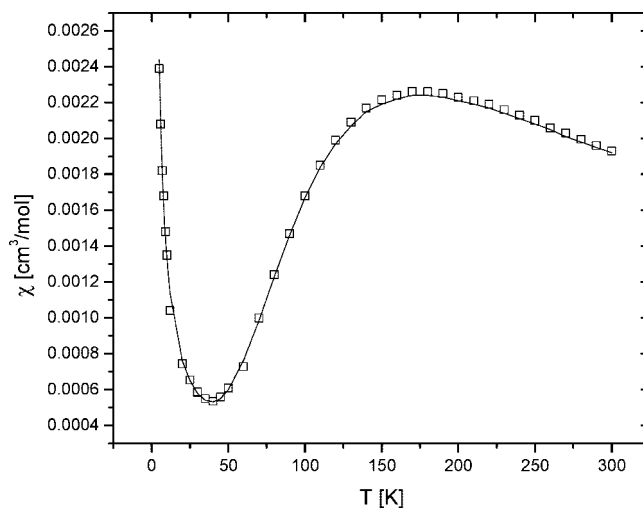


Figure 8. χ vs T plot for $(\text{Cp}''_2\text{Ti})_2(\text{N}_2)$. The g value was fixed as the value obtained from the EPR study ($g_{\text{av}} = 1.9777$); the Curie constant C was set to 0.3298 as determined from the χ vs $1/T$ plot of $\text{Cp}''_2\text{TiCl}$. The parameters were obtained from a least-squares refinement: $J/k = -144 \text{ K}$ (-100 cm^{-1}), $x_p = 3.4\%$, TIP $1.98 \times 10^{-4} \text{ cm}^3/\text{mol}$, and $-2J = 288 \text{ K}$ (200 cm^{-1}).

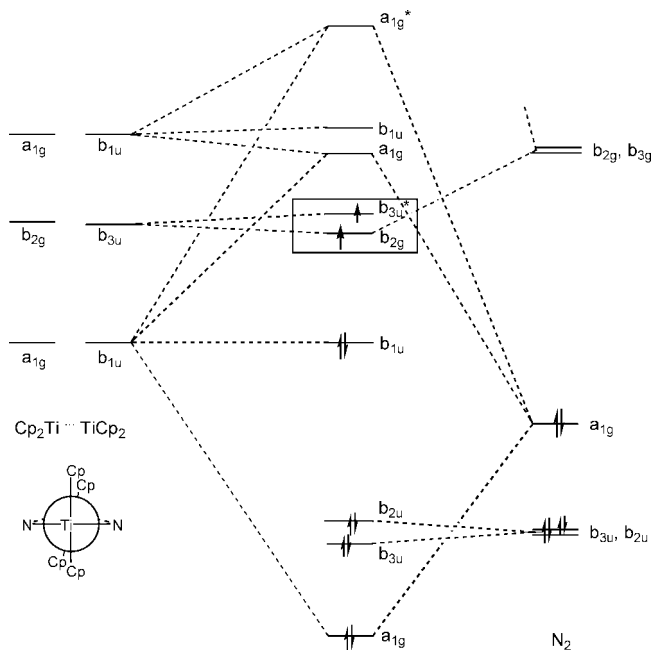


Figure 9. Qualitative molecular orbital diagram for $(\text{Cp}_2\text{Ti})_2(\text{N}_2)$ in D_{2h} symmetry.

from $\text{Cp}'_2\text{Ti}$ and one orbital from N_2). A qualitative MO diagram is shown in Figure 9.

In this model, bonding mainly occurs by way of the a_{1g} lone pair on N_2 and the $\text{Cp}'_2\text{Ti}$ a_{1g} symmetry orbitals, and the π -donation and π -back-bonding are poor in these systems, which stabilizes the b_{3u} orbital, while the b_{2g} orbital is slightly destabilized. This qualitative model is supported by molecular orbital calculations.³⁷ The four metal-based electrons are located in the b_{1u} and b_{2g} or b_{3u}^* orbital, leading to a small singlet–triplet splitting and antiferromagnetic coupling between the spin carriers as observed at low temperature in the solid state magnetism (Figures 6 and 8). The required reorganization energy

(36) Ren, Q.; Chen, Z.; Ren, J.; Wei, H.; Feng, W.; Zhang, L. *J. Phys. Chem. A* **2002**, *106*, 6161–6166.

(37) Blomberg, M. R. A.; Siegbahn, P. E. M. *J. Am. Chem. Soc.* **1993**, *115*, 6908–6915.

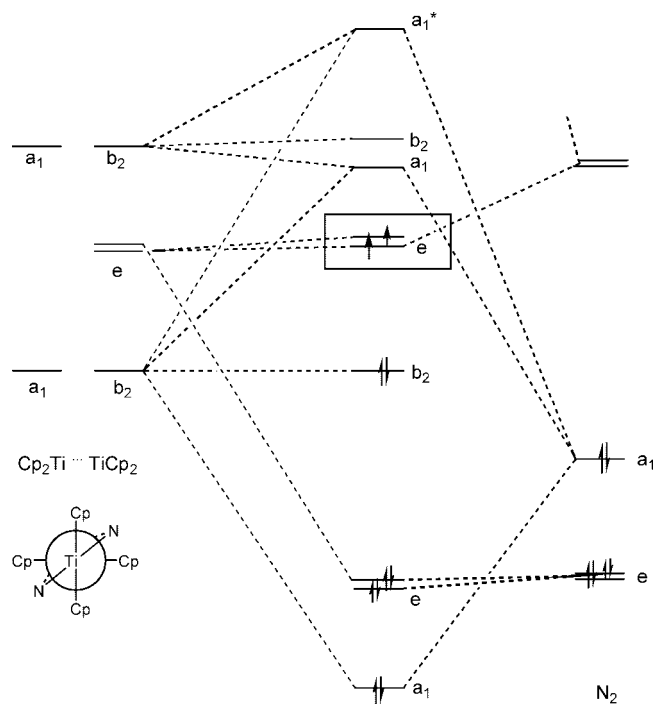


Figure 10. Qualitative molecular orbital diagram for $(\text{Cp}_2\text{Ti})_2(\text{N}_2)$ in D_{2d} symmetry.

is small, since the electrons are delocalized over three orbitals, exhibiting only minor electron–electron repulsion. A qualitative molecular orbital diagram for the D_{2d} symmetric $[(\text{C}_5\text{Me}_5)_2\text{Ti}]_2(\text{N}_2)$ is shown in Figure 10. In this case, the two electrons reside in a degenerate e orbital; the electrons are uncoupled and give rise to a spin triplet ($S = 1$), for which a magnetic moment of $\mu_{\text{eff}} = 2.83 \mu_{\text{B}}$ (per dimer) is expected. This prediction is consistent with the magnetism observed for $[(\text{C}_5\text{Me}_5)_2\text{Ti}]_2(\text{N}_2)$, which has a magnetic moment of $3.08 \mu_{\text{B}}$ (per dimer), and no electron exchange coupling from 20 to 260 K is observed.²⁹ Thus, the magnetic results may be rationalized by the symmetry of the metal-based fragment orbitals, which are determined by the orientation of the metallocene fragments.

The ^1H NMR spectrum of $(\text{Cp}''_2\text{Ti})_2(\text{N}_2)$ presents a puzzle, since it is temperature and time dependent. A freshly crystallized sample dissolved in C_6D_6 at 21 °C shows two resonances at 2.65 ppm ($\nu_{1/2} = 160$ Hz) and 5.3 ppm ($\nu_{1/2} = 44$ Hz), in the intensity ratio 96:4 assigned to the SiMe_3 groups. The freshly crystallized sample of $(\text{Cp}''_2\text{Ti})_2(\text{N}_2)$ dissolved in C_7D_8 , and cooled to -30 °C, was exposed to dynamic vacuum, while flame sealing the NMR tube. The NMR spectrum, collected at 290 K, contains the two signals in an intensity ratio of 87:13. Heating the sample to 353 K results in both signals moving to high field; however, the signal at 5.3 ppm gains intensity at the expense of the signal at 2.65 ppm. At 348 K, the intensities are roughly inverted compared to their ratio at 290 K. But, the original ratio is not obtained on cooling to 288 K; the peak at 5.3 ppm remains dominant, while the resonance at 2.65 ppm appears as two separated signals, a very broad one at 2.73 ppm and a relatively sharp one at 2.09 ppm, which overlaps with the toluene solvent resonance. The intensity ratio of the 5.3 ppm resonance to the 2.73 and 2.09 ppm pair is 54:46. The origin of this unusual behavior is unclear; however it can be reproduced using a freshly prepared sample. The ratio is also influenced by the way the

sample is treated, i.e., if it was cooled and then heated or first heated then cooled.³⁸

Given the unusual behavior of $(\text{Cp}''_2\text{Ti})_2(\text{N}_2)$, the NMR behavior of $(\text{Cp}'_2\text{Ti})_2(\text{N}_2)$ was investigated. At room temperature, one dominant signal at 3.60 ppm ($\nu_{1/2} = 60$ Hz) is observed, which overlaps a very broad resonance at 3.2 ppm ($\nu_{1/2} \approx 160$ Hz). An exact integration is difficult, since the resonances overlap, but it is on the order of 10:1. The ratio is not strongly affected when the sample is prepared under argon or nitrogen atmosphere. The chemical shifts are close to that of base-free $\text{Cp}'_2\text{Ti}$, and the absence of $\text{Cp}'_2\text{TiCl}$ is confirmed by EPR spectroscopy. When the sample is heated to 373 K, the signal at 3.2 ppm disappears, while the 3.6 ppm resonance shifts to higher field. At 368 K, only one signal at 2.52 ppm ($\nu_{1/2} = 40$ Hz) is detected, and on cooling, the original ratio is roughly restored. Low-temperature NMR studies are problematic due to the low solubility of both N_2 adducts. Clearly, equilibria are present in solution in both compounds, but given the time and temperature dependence, a detailed molecular explanation is not possible.³⁸

2. Carbon Monoxide. Exposure of either the base-free or the N_2 adduct to CO yields $\text{Cp}'_2\text{Ti}(\text{CO})_2$ as red crystals from hexane. The adduct melts at 125–127 °C, gives a molecular ion in the mass spectrum, and is diamagnetic, as deduced by its ^1H NMR spectrum; see Experimental Section for details. The CO stretching frequencies are observed in the Nujol mull IR spectrum at 1960 and 1880 cm^{-1} . The corresponding values for $\text{Cp}_2\text{Ti}(\text{CO})_2$ and $(\text{C}_5\text{Me}_5)_2\text{Ti}(\text{CO})_2$ are 1977 and 1899 cm^{-1} and 1940 and 1858 cm^{-1} , respectively, consistent with the view that the electron density³⁹ on the metallocene fragment in $\text{Cp}'_2\text{Ti}(\text{CO})_2$ is intermediate between those of the Cp and Cp^* derivatives.⁴⁰ The ν_{CO} values for the dicarbonyl adducts $[1,3-(\text{Me}_3\text{C})_2\text{C}_5\text{H}_3]_2\text{Ti}(\text{CO})_2$ in Nujol and $[1,3-(\text{Me}_3\text{Si})_2\text{C}_5\text{H}_3]_2\text{Ti}(\text{CO})_2$ in C_6D_6 are identical,¹⁷ although they differ by 11 cm^{-1} in the corresponding zirconocene adducts, with the Me_3C derivatives being lower.⁴⁰ The dicarbonyl takes on a blue coloration on standing in a dinitrogen atmosphere for prolonged periods of time, presumably due to slow displacement of CO by N_2 .

3. Diphenylacetylene. Addition of diphenylacetylene to the titanocene gives the red, diamagnetic 1:1 adduct on crystallization from hexane. The adduct does not react with N_2 or ethylene at 1 atm of pressure. An ORTEP diagram is shown in Figure 11, and some bond lengths and angles are listed in Table 1. The bond distances and angles around the metallocene fragment are very close to those of $\text{Cp}'_2\text{TiCl}_2$. In both metallocenes, the Cp rings are eclipsed, and in the diphenylacetylene fragment the phenyl rings are bent away from C(33) and C(34) by an angle of 137° (averaged). The phenyl rings are twisted out of the plane formed by Ti, C(33), and C(34); the two dihedral angles formed by the intersections of the phenyl rings with the

(38) A referee suggested that the resonance at δ 2.65 may be assigned to the D_{2h} conformer and the one at δ 5.3 to the D_{2d} conformer, since the ratio irreversibly changes toward the δ 5.3 resonance, which is the least sterically congested conformer. Over time, the resonance at δ 2.65 evolved into two resonances, which might be due to various Cp'' ring conformations within the D_{2h} conformation. While we agree with the general postulate that isomers are present (see the next paragraph), we can provide no experimental evidence for the specific assignment. The solid state magnetic measurements might be useful, but they were obtained only to temperatures of 300 K; on cooling from 300 to 5 K, no obvious deviation from the original χ vs T plots were evident to the eye. We thank a referee for this suggestion.

(39) Sikora, D. J.; Moriarty, K. J.; Rausch, M. D. *Inorg. Synth.* **1986**, *24*, 147–156.

(40) Zachmanoglou, C. E.; Docrat, A.; Bridgewater, B. M.; Parkin, G.; Brandow, C. G.; Bercaw, J. E.; Jardine, C. N.; Lyall, M.; Green, J. C.; Keister, J. B. *J. Am. Chem. Soc.* **2002**, *124*, 9525–9546.

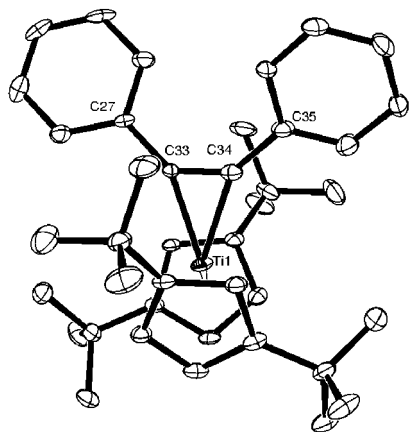


Figure 11. ORTEP diagram of $[1,3-(\text{Me}_3\text{C})_2\text{C}_5\text{H}_3]_2\text{Ti}(\text{PhCCPh})$ (30% probability ellipsoids). Hydrogen atoms have been omitted for clarity.

plane are 23° and 24° . The solid state structure is very similar to that found for $\text{Cp}_2\text{Ti}(\text{PhCCSiMe}_3)$ and $(\text{C}_5\text{Me}_5)_2\text{Ti}(\text{PhCCSiMe}_3)$.⁴¹

4. Ethylene. Exposure of $\text{Cp}'_2\text{Ti}$ to ethylene (1 atm of pressure) results in a rapid color change from blue to yellow, and a green-yellow 1:1 adduct may be obtained from hexane on cooling. The adduct melts at $122\text{--}123^\circ\text{C}$, but does not yield a molecular ion in the mass spectrum; only a molecular ion due to $\text{Cp}'_2\text{Ti}$ is observed. The adduct is diamagnetic and has averaged C_{2v} symmetry by ^1H and ^{13}C NMR spectroscopy at 23°C . When an excess of C_2H_4 is added to the C_6D_6 solution of $\text{Cp}'_2\text{Ti}(\text{C}_2\text{H}_4)$, resonances due to the two individual components are observed and no intermolecular exchange occurs on the ^1H NMR time scale. This is in contrast to $(\text{C}_5\text{Me}_5)_2\text{Ti}(\text{C}_2\text{H}_4)$, which exchanges with added C_2H_4 at room temperature.⁴² Exposure of $\text{Cp}'_2\text{Ti}(\text{C}_2\text{H}_4)$ to 1 atm of N_2 in C_6D_6 leads to a color change from yellow-green to blue-green, and in the ^1H NMR spectrum resonances of both species $\text{Cp}'_2\text{Ti}(\text{C}_2\text{H}_4)$ and $(\text{Cp}'_2\text{Ti})_2(\text{N}_2)$ can be detected in a ratio of approximately 10:1 at 20°C .

An ORTEP diagram of the ethylene adduct is shown in Figure 12, and important bond distances and angles are listed in Table 1. The molecular geometry is essentially identical to that of $(\text{C}_5\text{Me}_5)_2\text{Ti}(\text{C}_2\text{H}_4)$ ⁴² and close to that of $(\text{C}_5\text{Me}_4\text{SiMe}_3)_2\text{Ti}(\text{C}_2\text{H}_4)$.⁸ The hydrogen atoms on the ethylene group were located in the Fourier electron density map and refined isotropically. This allows the bend angle, α , as defined by Stalick and Ibers, of 60° to be calculated.^{43,44} This angle, the strong bending observed in the diphenylacetylene adduct, and the ν_{CO} 's in the CO adduct clearly indicate that the $[1,3-(\text{Me}_3\text{C})_2\text{C}_5\text{H}_3]_2\text{Ti}$ fragment is a good π -donor.

5. Dihydrogen. Perhaps the most interesting reaction of $\text{Cp}'_2\text{Ti}$ is its reaction with dihydrogen. Exposure of $\text{Cp}'_2\text{Ti}$ in C_6D_6 to an atmosphere of dihydrogen in an NMR tube results in a rapid color change from blue to brown-red; exposure of this solution to vacuum regenerates the blue color. This cycle can be repeated several times. On a synthetic scale, cooling the brown-red hexane solution to -80°C yields dark red crystals that are stable to vacuum in the solid state. The dihydride melts

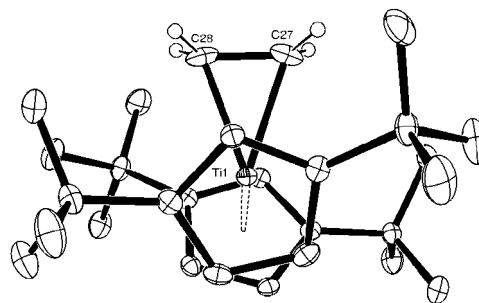


Figure 12. ORTEP diagram of $[1,3-(\text{Me}_3\text{C})_2\text{C}_5\text{H}_3]_2\text{Ti}(\text{H}_2\text{CCH}_2)$ (30% probability ellipsoids). All hydrogen atoms were located; the hydrogen atoms on the Me_3C groups and methine positions of the cyclopentadienyl ligand were included in calculated positions using a riding model, but not refined. The hydrogen atoms are omitted for clarity, except the hydrogen atoms on the ethylene ligand, which were refined isotropically.

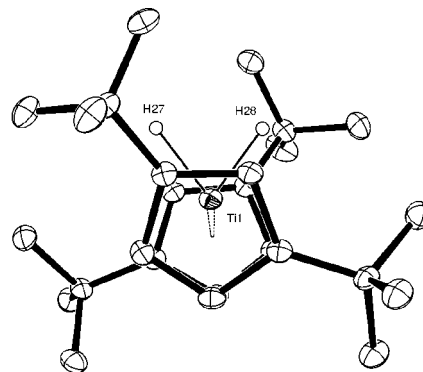


Figure 13. ORTEP diagram of $[1,3-(\text{Me}_3\text{C})_2\text{C}_5\text{H}_3]_2\text{TiH}_2$ (30% probability ellipsoids). All of the hydrogen atoms were located; the hydrogen atoms on the Me_3C groups and methine positions of the cyclopentadienyl ligand were included in calculated positions using a riding model, but not refined. For clarity, all hydrogens are omitted except the hydrides (H27, H28), which were refined isotropically.

at $152\text{--}154^\circ\text{C}$, but no molecular ion is observed in the mass spectrum, only that due to $\text{Cp}'_2\text{Ti}$ is observed. The IR spectrum shows a broad, strong feature at 1640 cm^{-1} assigned to $\nu_{\text{Ti-H}}$, since in $(\text{C}_5\text{Me}_5)_2\text{TiH}_2$, $\nu_{\text{Ti-H}}$ is observed at 1560 cm^{-1} .⁴⁵ Crystals suitable for an X-ray diffraction study may be grown from a dihydrogen-saturated solution of $\text{Cp}'_2\text{Ti}$ in hexane; an ORTEP diagram is shown in Figure 13, and some bond distances and angles are listed in Table 1. The hydrogen atoms, H(27 and 28), were located in the difference map and refined isotropically. The orientation of the rings is staggered, as they are in $\text{Cp}'_2\text{Ti}(\text{PhCCPh})$, Figure 11. The Ti-H distances of $1.58(3)$ and $1.63(3)\text{ \AA}$ are comparable to the X-ray determined distances of $1.69(5)$ and $1.84(4)\text{ \AA}$ for the two independent $(\text{C}_5\text{Me}_5)_2\text{TiH}$ molecules,¹⁰ $1.77(2)\text{ \AA}$ in $(\text{C}_5\text{Me}_4\text{Ph})_2\text{TiH}$,¹¹ and $1.84(2)\text{ \AA}$ in the recently reported cation $\{(\text{C}_5\text{Me}_5)_3\text{Ti}[\text{NP}(\text{CMe}_3)_3][\text{thf}][\text{H}]\}^+$.⁴⁶ The HTiH angle of $72(2)^\circ$ also seems reasonable, since a HMOH angle of $75.5(3)^\circ$ is found in Cp_2MoH_2 in a neutron diffraction study.⁴⁷

As mentioned above, $\text{Cp}'_2\text{Ti}$ undergoes a reversible color change when exposed to H_2 , and this reaction may be monitored

(41) Burlakov, V. V.; Polyakov, A. V.; Yanovsky, A. L.; Struchkov, Y. T.; Shur, V. B.; Volpin, M. E.; Rosenthal, U.; Görls, H. *J. Organomet. Chem.* **1994**, *476*, 197–206.

(42) Cohen, S. A.; Auburn, P. R.; Bercaw, J. E. *J. Am. Chem. Soc.* **1983**, *105*, 1136–1143.

(43) Stalick, J. K.; Ibers, J. A. *J. Am. Chem. Soc.* **1970**, *92*, 5333–5338.

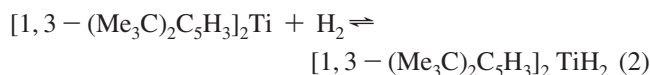
(44) Ittel, S. D.; Ibers, J. A. *Adv. Organomet. Chem.* **1976**, *14*, 33–61.

(45) Bercaw, J. E.; Marvich, R. H.; Bell, L. G.; Brintzinger, H. H. *J. Am. Chem. Soc.* **1972**, *94*, 1219–1238.

(46) Ma, K.; Piers, W. E.; Gao, Y.; Parvez, M. *J. Am. Chem. Soc.* **2004**, *126*, 5668–5669.

(47) Schultz, A. J.; Stearly, K. L.; Williams, J. M.; Mink, R.; Stucky, G. D. *Inorg. Chem.* **1977**, *16*, 3303.

by ^1H NMR spectroscopy. At 30 °C, the blue solution of $\text{Cp}'_2\text{Ti}$ in C_6D_6 under argon shows a broad ($\nu_{1/2} = 300$ Hz) resonance at δ 3.2 ppm. Exposure of this solution to an atmosphere of H_2 results in a color change to brown-red and a slight upfield shift in the broad resonance. Cooling the sample to -10 °C results in the appearance of the broad resonance at δ 3.0 ppm, and four sharp resonances without structure appear upfield. Cooling to -55 °C results in the disappearance of the broad resonance, the four sharp features due to $\text{Cp}'_2\text{TiH}_2$ appear at δ 1.13 (CMe_3), and the A_2B ring resonances appear as a doublet at δ 5.10 ($J = 3$ Hz), a triplet at δ 8.01 ($J = 3$ Hz), and a singlet at δ 2.62 due to Ti-H increase in intensity. The chemical shift for the Ti-H resonance is intermediate between δ 0.28 in $(\text{C}_5\text{Me}_5)_2\text{TiH}_2$ ⁴⁵ and δ 3.25 in $(\text{C}_5\text{Me}_4\text{iPr})_2\text{TiH}_2$.⁴⁸ Returning the sample to 30 °C yields the original spectrum. This behavior implies an equilibrium, eq 2, which will have



a dependence on pressure of H_2 . Repeating the ^1H NMR experiment at 30 °C as a function of applied pressure of H_2 results in an upfield shift of the averaged chemical shift of the broadened resonance, presumably due to the averaged chemical shift of CMe_3 groups, until a sharp feature begins to appear at δ 1.5 at an applied pressure of about 30 psi, which sharpens and shifts upfield as the applied pressure is increased to about 160 psi. These shifts as a function of applied pressures are shown graphically as Supporting Information. The qualitative pressure dependence is consistent with the equilibrium reaction shown in eq 2. Unfortunately, the equilibrium reaction can be treated only semiquantitatively since, although the absolute chemical shifts of pure $\text{Cp}'_2\text{Ti}$ or $\text{Cp}'_2\text{TiH}_2$ are known accurately at a given temperature, that due to paramagnetic $\text{Cp}'_2\text{Ti}$ is very broad and temperature dependent. The dependence of the equilibrium on the applied pressure of H_2 may be estimated from the ratios of the populations of the two titanocenes and the solubility of H_2 at 30 °C in toluene,⁴⁹ as $K_p(303\text{ K}) = 29.1(2)\text{ bar}^{-1}$ (see Supporting Information for details). For $(\text{C}_5\text{Me}_5)_2\text{Ti}$ a value of $K_p(300\text{ K}) \approx 100\text{ bar}^{-1}$ was determined,⁴⁵ which is consistent with the notion that the $\text{Cp}'_2\text{Ti}$ binds H_2 less strongly than does the $(\text{C}_5\text{Me}_5)_2\text{Ti}$ fragment.

The reversible reaction illustrated in eq 2 is of synthetic utility, since the purest form of $\text{Cp}'_2\text{Ti}$ is obtained by allowing crystalline $\text{Cp}'_2\text{TiH}_2$ to decompose by gently warming a solution in hexane, which is in contrast to the published observations on $(\text{C}_5\text{Me}_5)_2\text{TiH}_2$ ²⁵ and $(\text{C}_5\text{Me}_4\text{iPr})_2\text{TiH}_2$,⁴⁸ in both of these cases H_2 elimination leads to the formation of Ti(III) hydrides.

6. N_2O . Synthesis and reactions of metal oxides and hydroxide complexes have been of interest to us in recent years.^{1,50–52} Nitrous oxide is a convenient source of oxygen atoms for the synthesis of oxometallocenes (and the products derived therefrom) as well as for the insertion into metal-hydrogen and -carbon bonds.^{53–56} Alternatively, ethylene oxide or styrene

(48) Hanna, T. E.; Lobkovsky, E.; Chirik, P. J. *Eur. J. Inorg. Chem.* **2007**, 2677–2685.

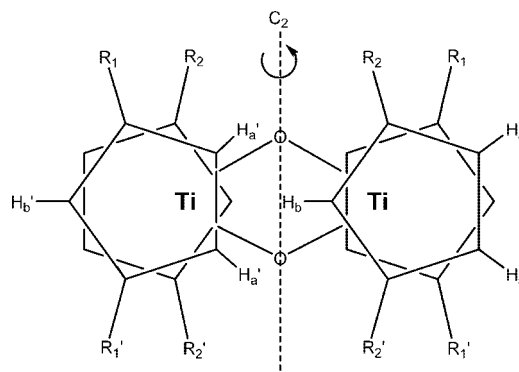
(49) Lühring, P.; Schumpe, A. *J. Chem. Eng. Data* **1989**, *34*, 250–252.

(50) Polse, J. L.; Andersen, R. A.; Bergman, R. G. *J. Am. Chem. Soc.* **1995**, *117*, 5393–5394.

(51) Schwartz, D. J.; Smith, M. R.; Andersen, R. A. *Organometallics* **1996**, *15*, 1446–1450.

(52) Zi, G.; Li, J.; Werkema, E. L.; Walter, M. D.; Gottfriedsen, J. P.; Andersen, R. A. *Organometallics* **2005**, *24*, 4251–4264.

(53) Bottomley, F.; Egharevba, G. O.; Lin, I. J. B.; White, P. S. *Organometallics* **1985**, *4*, 550–553.



Idealized C_{2h} symmetry inferred from NMR data

Figure 14. Cp' ring conformation in the $\text{Cp}'_4\text{Ti}_2(\mu\text{-O})_2$ dimer.

oxide have been used as O-atom transfer reagents to prepare monomeric, base-free titanocene oxides.⁵⁷ Accordingly, the reaction of $\text{Cp}'_2\text{Ti}$ and $\text{Cp}'_2\text{Ti}(\text{C}_2\text{H}_4)$ toward nitrous oxide, N_2O , was studied. On exposure of $\text{Cp}'_2\text{Ti}$ to N_2O (1 atm of pressure) the oxo-bridged dimetal compound $\text{Cp}'_4\text{Ti}_2(\mu\text{-O})$ can be isolated, albeit in low yield, and the molecular structure was determined by X-ray diffraction.⁵⁸ Under the same conditions $(\text{C}_5\text{Me}_5)_2\text{Ti}$ yields a mixture of compounds, as indicated by ^1H NMR spectroscopy; resonances due to $[(\text{C}_5\text{Me}_5)\text{Ti}]_2[\mu\text{-}(\eta^1\text{-}\eta^5\text{-CH}_2\text{C}_5\text{Me}_4)](\mu\text{-O})_2$ ^{53,54} and for $(\text{C}_5\text{Me}_5)_4\text{Ti}_4(\mu\text{-O})_6$ ^{59,60} can be identified. Monomeric $(\text{C}_5\text{Me}_5)_2\text{Ti}(\text{O})(\text{py})$ may be isolated, if the reaction of $(\text{C}_5\text{Me}_5)_2\text{Ti}$ or $(\text{C}_5\text{Me}_5)_2\text{Ti}(\text{C}_2\text{H}_4)$ with N_2O is conducted in the presence of pyridine.⁶¹ However, on exposure of $\text{Cp}'_2\text{Ti}(\text{C}_2\text{H}_4)$ to N_2O (1 atm of pressure), the only identifiable product is the dimeric $\text{Cp}'_4\text{Ti}_2(\mu\text{-O})_2$, mp 228–229 °C. $\text{Cp}'_4\text{Ti}_2(\mu\text{-O})$ is not obtained by this synthetic methodology, since addition of 0.5 equiv of N_2O to a pentane solution of $\text{Cp}'_2\text{Ti}(\text{C}_2\text{H}_4)$ yields a mixture of $\text{Cp}'_4\text{Ti}_2(\mu\text{-O})_2$ and unreacted starting material. Although the microcrystalline nature of $\text{Cp}'_4\text{Ti}_2(\mu\text{-O})_2$ precluded a crystal structure analysis, the ^1H NMR data are consistent with a dimeric molecule of C_{2h} symmetry. Furthermore, its IR spectrum resembles that of the uranium analogue $\text{Cp}'_4\text{U}_2(\mu\text{-O})_2$, for which single-crystal and EXAFS data are available.¹ The ^1H NMR spectrum consequently shows inequivalent Cp' resonances (see Experimental Section), suggesting that the geometrical structure shown in Figure 14 is analogous to that found for its uranium analogue.

$\text{Cp}'_4\text{Ti}_2(\mu\text{-O})_2$ does not react with excess $\text{Cp}'_2\text{Ti}(\text{C}_2\text{H}_4)$ or 4-dimethylaminopyridine (DMAP), suggesting that the dimer does not dissociate, consistent with its ^1H NMR spectrum. Similar observations have been reported for $\text{Cp}''_4\text{Ti}_2(\mu\text{-O})_2$, which was prepared from $\text{Cp}''_2\text{Ti}=\text{NR}$ and Ph_2CO .¹⁷

Conclusions

The introduction of the 1,3-di-*tert*-butylcyclopentadienyl ligand into titanium chemistry allows the isolation of base-free

(54) Bottomley, F.; Lin, I. J. B.; White, P. S. *J. Am. Chem. Soc.* **1981**, *103*, 703–704.

(55) Bottomley, F.; Lin, I. J. B.; Mukaida, M. *J. Am. Chem. Soc.* **1980**, *102*, 5238–5242.

(56) Matsunaga, P. T.; Moropoulos, J. C.; Hillhouse, G. L. *Polyhedron* **1995**, *14*, 175–185, and references therein.

(57) Hanna, T. E.; Lobkovsky, E.; Chirik, P. J. *Inorg. Chem.* **2007**, *46*, 2358–2361.

(58) Sofield, C. D.; Walter, M. D.; Andersen, R. A. *Acta Crystallogr. E* **2004**, *60*, m1417–m1419.

(59) Babcock, L. M.; Day, V. W.; Klemperer, W. G. *J. Chem. Soc., Chem. Commun.* **1987**, 858.

(60) Babcock, L. M.; Klemperer, W. G. *Inorg. Chem.* **1989**, *28*, 2003.

(61) Smith, M. R.; Matsunaga, P. T.; Andersen, R. A. *J. Am. Chem. Soc.* **1993**, *115*, 7049–7050.

$\text{Cp}'_2\text{Ti}$, which reacts with a variety of substrates in analogy with $(\text{C}_5\text{Me}_5)_2\text{Ti}$. The purity of the base-free titanocene can easily be determined by EPR and UV-vis spectroscopy. The reaction with N_2 gives the 2:1 complex $(\text{Cp}'_2\text{Ti})_2(\text{N}_2)$, in which the titanium centers are strongly antiferromagnetically coupled. Although a crystal structure was not obtained, the magnetic behavior is essentially identical to its $(\text{Cp}''_2\text{Ti})_2(\text{N}_2)$ analogue, whose X-ray crystal structure is known, in which the two titanocene units are related by inversion with the inversion center located in the middle of the N-N bond; this allows effective antiferromagnetic coupling via the N_2 bridge. This is in contrast to Bercaw's observations on $[(\text{C}_5\text{Me}_5)_2\text{Ti}]_2(\text{N}_2)$, in which the titanium centers are twisted by 90° relative to each other, and consequently only weak coupling is allowed. $\text{Cp}'_2\text{Ti}(\text{C}_2\text{H}_4)$, which is generated from $\text{Cp}'_2\text{Ti}$ and C_2H_4 , is a convenient starting material for the synthesis of dimeric $\text{Cp}'_4\text{Ti}_2(\mu\text{-O})_2$ species with C_{2h} symmetry, as judged from its ^1H NMR spectrum. $\text{Cp}'_2\text{TiCl}$ can be functionalized with MeLi to give $\text{Cp}'_2\text{TiMe}$, which reacts with H_2 and H_2O to yield monomeric $\text{Cp}'_2\text{TiH}$ and $\text{Cp}'_2\text{TiOH}$, respectively.

Experimental Section

General Comments. All reactions, product manipulations, and physical studies have been carried out as previously described.^{10,62–65}

$\text{Cp}'_2\text{TiCl}$. Tetrahydrofuran (150 mL) was added to a mixture of $\text{TiCl}_3 \cdot 3\text{THF}$ (13.0 g, 34.9 mmol) and $\text{Cp}'_2\text{Mg}$ (13.2 g, 34.9 mmol). The solution turned dark blue immediately, and the mixture was stirred for 12 h. The solvent was removed under reduced pressure, and the resulting dark blue solid was extracted with 2×150 mL of hexane. The combined extracts were concentrated to a volume of 200 mL and cooled to -80°C . Blue needles were isolated (11.6 g, 83% yield). Mp: 145–146 $^\circ\text{C}$. ^1H NMR (C_6D_6 , 21°C): δ 3.8 ($\nu_{1/2} = 430$ Hz). IR (Nujol mull; CsI windows; cm^{-1}): 3110(w), 3090(w), 1393(m), 1372(s), 1364(m), 1357(s), 1294(m), 1253(s), 1197(m), 1166(m), 1059(s), 1035(w), 1028(w), 935(w), 928(w), 919(w), 885(w), 878(w), 846(s), 821(w), 808(m), 720(w), 680(w), 655(m), 498(m), 453(m), 342(w), 325(w), 274(m). UV-vis (methylcyclohexane, 25°C): 625 nm ($\epsilon = 96$ L mol $^{-1}$ cm $^{-1}$), 560 nm ($\epsilon = 107$ L mol $^{-1}$ cm $^{-1}$). Anal. Calcd for $\text{C}_{26}\text{H}_{42}\text{ClTi}$: C, 71.31; H, 9.67. Found: C, 71.04; H, 9.57. The EI mass spectrum showed a parent ion at $m/e = 437$ amu. The parent ion isotopic cluster was simulated (calcd %, obsvd %): 435 (10, 13), 436 (12, 15), 437 (100, 100), 438 (44, 47), 439 (53, 44), 440 (14, 17), 441 (5, 5), 442 (1, 1).

$\text{Cp}'_2\text{TiCl}_2$. Carbon tetrachloride (5 mL, 50 mmol) was dissolved in tetrahydrofuran (100 mL), and the solution was added to $\text{Cp}'_2\text{TiCl}$ (4.48 g, 10.2 mmol) and stirred for 8 h. The dark blue solution gradually changed to red, and red needles deposited, which were collected (4.32 g, 89% yield). Mp: 223–225 $^\circ\text{C}$. ^1H NMR (C_6D_6 , 21°C): δ 1.29 (s, 36 H, $\text{C}(\text{CH}_3)_3$), 5.81 (d, 4H, $^4J_{\text{CH}} = 3$ Hz, ring-CH), 6.77 ppm (t, 2H, $^4J_{\text{CH}} = 3$ Hz, ring-CH).

A second method: Tetrahydrofuran (250 mL) was added to mixture of $\text{Cp}'_2\text{TiCl}$ (7.33 g, 16.7 mmol) and HgCl_2 (5.00 g, 18.4 mmol). A dark red solution with a colorless precipitate immediately formed. The mixture was stirred for 3 h, and the solvent was removed under reduced pressure. The dark red product was sublimed (150 $^\circ\text{C}$, 10^{-3} Torr) and crystallized from tetrahydrofuran. The compound has been prepared by other methods.^{3,4}

$\text{Cp}'_2\text{TiMe}$. Diethyl ether (50 mL) was added to $\text{Cp}'_2\text{TiCl}$ (3.9 g, 8.8 mmol). Methylolithium in diethyl ether (11 mL, 0.81 M, 8.8

mmol) was added to the blue solution using a syringe. The solution immediately turned green, and a colorless solid precipitated. The solvent was removed under reduced pressure and the green solid was extracted with hexane (50 mL). The solution was filtered, concentrated to a volume of 25 mL, and cooled to -20°C . The green crystals (1.24 g) were isolated by filtration, and the mother liquor was concentrated and cooled to -80°C . Total yield: 2.14 g (58%). The isolated crystals gave negative Li flame and negative AgNO_3 tests. Purification can also be accomplished by sublimation in diffusion pump vacuum at $60\text{--}70^\circ\text{C}$. Mp: 128–129 $^\circ\text{C}$ (rev). ^1H NMR (C_6D_6 , 21°C): δ 3.61 ($\nu_{1/2} = 430$ Hz). IR (Nujol mull; CsI windows, cm^{-1}): 1297(w), 1252(s), 1238(w), 1200(m), 1168(m), 1108(w), 1062(m), 1023(m), 939(m), 931(m), 844(s), 820(w), 812(w), 802(m), 791(s), 721(w), 680(w), 658(s), 605(w), 495(w), 442(w), 387(w), 310(w). Anal. Calcd for $\text{C}_{27}\text{H}_{45}\text{Ti}$: C, 77.7; H, 10.86. Found: C, 77.58; H, 11.13.

An alternative method: Methylolithium (11 mL, 0.81 M in Et_2O , 8.8 mmol) was added dropwise to an ether suspension of $\text{Cp}'_2\text{TiCl}_2$ (2.0 g, 4.2 mmol). The dark red suspension changed to a light green with a colorless precipitate. The mixture was stirred for 30 min, and the solvent was removed under reduced pressure. The solid was extracted with hexane (100 mL), and the green solution was filtered and concentrated to a volume of 40 mL and cooled to -80°C . Green needles of $\text{Cp}'_2\text{TiMe}$ were isolated (identified by its IR spectrum and mp).

$\text{Cp}'_2\text{TiOH}$. Toluene (50 mL) was added to $\text{Cp}'_2\text{TiMe}$ (1.3 g, 3.1 mmol). A solution of degassed water (56 μL , 3.1 mmol) in 30 mL of tetrahydrofuran was added to the green $\text{Cp}'_2\text{TiMe}$ solution via cannula. The mixture was heated gently to $35\text{--}40^\circ\text{C}$ for 15 min. During this time the color changed to light blue-purple and gas evolved. The solvent was removed under reduced pressure, and the residue was extracted into pentane (30 mL). The pentane solution was concentrated and cooled to -25°C to give blue-purple blocks (0.73 g, 1.74 mmol, 56%). Mp: 110–112 $^\circ\text{C}$ (rev). ^1H NMR (C_6D_6 , 21°C): δ 3.66 ($\nu_{1/2} = 670$ Hz). IR (Nujol mull; CsI windows, cm^{-1}): 3668(s), 3080(w), 1595(w), 1392sh.(m), 1375(s), 1360(s), 1300(w), 1258(s), 1205(m), 1170(m), 1090(vbr m), 1060(vbr m), 1030(vbr m), 940(vbr m), 890(br w), 855(m), 842(vs), 815(m), 796(s), 730(vbr.w), 690(w), 680(w), 660(m), 630(br w), 590'(br vs), 595(sh), 500(w), 445(vbr m), 390(m), 340(w). Anal. Calcd for $\text{C}_{26}\text{H}_{43}\text{TiO}$: C, 74.44; H, 10.33. Found: C, 74.63; H, 10.59. The EI mass spectrum showed a parent ion at $m/e = 419$ amu. The parent ion isotopic cluster was simulated (calcd %, obsvd %): 417 (10, 9), 418 (13, 12), 419 (100, 100), 420 (37, 37), 421 (14, 14), 422 (3, 3).

$\text{Cp}'_2\text{TiH}$. Hexane (50 mL) was added to $\text{Cp}'_2\text{TiMe}$ (1.3 g, 3.1 mmol), and the green solution was exposed to 1 atm of hydrogen. The solution turned dark red in color within 5 min. The volume of the solution was reduced to 10 mL. Slow cooling to -80°C under a nitrogen atmosphere yielded brick-red crystals (1.04 g, 2.57 mmol, 83% yield). Solutions of $\text{Cp}'_2\text{TiH}$ show thermochromic behavior; they are red at room temperature and deep blue at -80°C . Mp: 147–149 $^\circ\text{C}$ (rev). ^1H NMR (C_6D_6 , 21°C): δ 2.68 ($\nu_{1/2} = 140$ Hz). IR (Nujol mull; CsI windows, cm^{-1}): 1550(s) (Ti-H), 1375(s), 1355(s), 1297(m), 1233(w), 1200(m), 1165(m), 1050(m), 1025(w), 945(w), 935(w), 927(m), 852(w), 837(s), 810(m), 781(w), 772(m), 723(m), 690(m), 659(m), 610(w), 585(w), 500(w), 470(m), 397(m), 320(w), 250(w). Anal. Calcd for $\text{C}_{26}\text{H}_{43}\text{Ti}$: C, 77.39; H, 10.74. Found: C, 77.22; H, 10.92.

$(\text{Cp}'\text{-d}_{18})_2\text{TiD}$. Pentane (50 mL) was added to $\text{Cp}'_2\text{TiMe}$ (0.3 g, 0.72 mmol), and the green solution was exposed to 9 atm of D_2 for 6 days; the atmosphere was exchanged once during this time period. The solution turned dark red in color within 5 min. The volume of the solution was reduced to 10 mL. Slow cooling to -80°C under a nitrogen atmosphere yielded brick-red crystals (0.2 g). ^2H NMR ($\text{C}_6\text{D}_6/\text{C}_6\text{H}_6$, 21°C): δ 2.69 ($\nu_{1/2} = 5$ Hz). IR (Nujol mull; CsI windows, cm^{-1}): 3080(w), 2210(vs) (C-D),

(62) Schultz, M.; Boncella, J. M.; Berg, D. J.; Tilley, T. D.; Andersen, R. A. *Organometallics* **2002**, *21*, 460–472.

(63) Walter, M. D.; Schultz, M.; Andersen, R. A. *New J. Chem.* **2006**, *30*, 238–246.

(64) Walter, M. D.; Berg, D. J.; Andersen, R. A. *Organometallics* **2006**, *25*, 3228–3237.

(65) Lukens, W. W.; Andersen, R. A. *Inorg. Chem.* **1995**, *34*, 3440–3443.

2110(br m) (C-D), 2060(m) (C-D), 2040(m) (C-D), 1530(vbr m), 1460(s), 1378(s), 1290(w), 1260(w), 1215(s), 1170(m), 1120(s) (Ti-D), 1100(w), 1052(w), 1025(m), 912(w), 902(m), 845(vs), 838(sh), 818(w), 780(vs), 750(m), 710(w), 707(w), 672(m), 648(m), 600(vw), 482(m), 467(m).

Cp₂Ti. Under argon, potassium amalgam was prepared from 20 mL of mercury and potassium (4.6 g, 120 mmol). Cp₂TiCl (10.3 g, 23.5 mmol) was dissolved in hexane (200 mL), and the solution was added to the potassium amalgam. The mixture was heated to reflux and stirred for 12 h. The stirring was halted, and the mixture was allowed to cool to room temperature. The dark blue solution was filtered and concentrated to a volume of 100 mL. Layered crystals formed (3.85 g, 41% yield). A second crop of crystals was obtained by concentrating and cooling the solution to -80 °C (2.5 g, 67% overall yield). Using the silver nitrate test, no chloride was detected either in the crystals or in mother liquor. Mp: 148–149 °C. ¹H NMR (C₆D₆, 30 °C): δ 3.2 (ν_{1/2} = 300 Hz). IR (Nujol mull; CsI windows, cm⁻¹): 3105(w), 3095(m), 1489(m), 1413(m), 1382(m), 1369(s), 1362(s), 1354(w), 1318(w), 1315(w), 1271(w), 1253(s), 1202(m), 1187(s), 1098(s), 1070(m), 1061(m), 1029(m), 948(s), 923(s), 904(w), 899(w), 867(s), 835(s), 760(s), 728(w), 700(m), 682(w), 673(w), 640(m), 591(w), 495(w), 470(w), 440(s), 420(m), 410(s), 377(w), 365(w), 338(w), 268(s). UV-vis (methylcyclohexane, 25 °C): 589 nm (ε = 121 L mol⁻¹ cm⁻¹). Anal. Calcd for C₂₆H₄₂Ti: C, 77.59; H, 10.52. Found: C, 77.29; H, 10.29. The EI mass spectrum showed a parent ion at *m/e* = 402 amu. The parent ion isotopic cluster was simulated (calcd %, obsvd %): 405 (3, 3), 404 (13, 17), 403 (36, 45), 402 (100, 100), 401 (13, 17), 400 (11, 14), 399 (0, 2).

An alternative method: High-purity Cp₂Ti may be easily obtained by allowing crystalline Cp₂TiH₂ to decompose into Cp₂Ti and H₂ by gently warming a solution in hexane.

(Cp₂Ti)(N₂). Cp₂Ti (1.0 g, 2.5 mmol) was dissolved in hexane (25 mL), and the solution was exposed to 1 atm of nitrogen. The solution was cooled to -78 °C, and very dark crystals with metallic golden luster formed (0.78 g, 75% yield). The compound appears homogeneous and blue when crushed in a mortar. Mp (under N₂ loss): 130–140 °C. The isolated crystals gave a negative AgNO₃ test. ¹H NMR (C₆D₆, 21 °C): δ 3.6 (ν_{1/2} = 60 Hz). IR (Nujol mull; CsI windows, cm⁻¹): 1300(m), 1255(s), 1235(w), 1210(m), 1200(m), 1170(s), 1055(w), 1050(m), 1020(m), 950(m), 940(w), 855(s), 830(s), 815(m), 785(s), 740(w), 725(w), 670(m), 660(m), 590(w), 500(w), 460(w), 405(w). UV-vis (methylcyclohexane, 25 °C): 603 nm (ε = 1850 L mol⁻¹ cm⁻¹). Anal. Calcd for C₂₆H₄₂N₂Ti: C, 74.98; H, 10.16; N, 3.36. Found: C, 74.88; H, 10.19; N, 3.43. The EI mass spectrum is consistent with Cp₂Ti.

An alternative method: Under nitrogen, potassium amalgam was prepared from 5 mL of mercury and potassium (1.2 g, 31 mmol). Cp₂TiCl (2.95 g, 6.76 mmol) was dissolved in toluene (60 mL), and the solution was added to the potassium amalgam. The mixture was heated to reflux and stirred for 12 h. The stirring was halted, and the mixture was allowed to cool to room temperature. The solvent was removed under vacuum, and the blue residue was extracted into 80 mL of pentane. The royal blue solution was cooled to -20 °C, affording very dark blue crystals with a metallic golden luster (1.75 g, 2.1 mmol, 62% yield).

Cp₂TiCl. Tetrahydrofuran (150 mL) was added to a mixture of TiCl₃·3THF (13.0 g, 34.9 mmol) and Cp^{''}₂Mg (15.5 g, 34.9 mmol). The solution turned dark blue immediately, and the mixture was stirred for 12 h. The solvent was removed under reduced pressure, and the resulting dark blue solid was extracted with 2 × 150 mL of hexane. The combined extracts were concentrated to a volume of 200 mL and cooled to -80 °C. Blue needles were isolated (14.9 g, 85% yield). Mp: 153–154 °C. ¹H NMR (C₆D₆, 21 °C): δ 2.66 (ν_{1/2} = 340 Hz). IR (Nujol mull; CsI windows, cm⁻¹): 3100(sh), 3090(s), 1940(br vw), 1880(br vw), 1830(w), 1805(w), 1760(w), 1460(vs), 1450(v), 1425(m), 1408(s), 1392(m), 1382(m),

1330(m), 1250(vbr s), 1210(vs), 1187(w), 1095(vs), 1070(m), 1060(s), 932(sh), 922(s), 870(s), 850(vbr s), 760(vs), 698v(s), 638v(s), 490(s), 438(s), 412(s), 383(s), 370(s), 350(vw), 300(s), 280(s), 258(m), 250(s). UV-vis (methylcyclohexane, 25 °C): 617 nm (ε = 72 L mol⁻¹ cm⁻¹), 550 nm (ε = 97 L mol⁻¹ cm⁻¹). Anal. Calcd for C₂₂H₄₂Si₄ClTi: C, 52.61; H, 8.43. Found: C, 52.33; H, 8.52.

(Cp^{''}₂Ti)(N₂). Under nitrogen, potassium amalgam was prepared from 5 mL of mercury and potassium (1.2 g, 31 mmol). Cp^{''}₂TiCl (2.95 g, 5.88 mmol) was dissolved in toluene (60 mL), and the solution was added to potassium amalgam. The mixture was heated to reflux and stirred for 12 h. The stirring was halted, and the mixture was allowed to cool to room temperature. The solvent was removed under reduced pressure, and the blue residue was extracted into 80 mL of pentane. The royal blue solution was cooled to -20 °C, affording very dark blue crystals with a metallic golden luster (1.9 g, 1.97 mmol, 67% yield). The compound appears homogeneous and blue when crushed in a mortar. Mp (under N₂ loss): 143–144 °C. The isolated crystals gave a negative AgNO₃ test. ¹H NMR (C₆D₆, 21 °C): δ 2.65 (ν_{1/2} = 170 Hz). IR (Nujol mull; CsI windows, cm⁻¹): 3080(vw), 1460(s), 1380(s), 1320(w), 1248(s), 1200(m), 1090(s), 923(s), 840(br vs), 810(m), 752(m), 725(w), 690(m), 638(m), 620(sh), 498(w), 485(w), 435(w), 390(m), 378(m), 360(w), 330(w), 268(m). UV-vis (methylcyclohexane, 25 °C): 614 nm (ε = 2500 L mol⁻¹ cm⁻¹). Anal. Calcd for C₄₄H₈₄N₂Si₈Ti₂: C, 54.96; H, 8.81; N, 2.91. Found: C, 54.67; H, 8.61; N, 2.62. The compound has been prepared by another method.¹⁷

Cp₂Ti(CO)₂. Cp₂Ti (1.0 g, 2.5 mmol) was dissolved in hexane (50 mL) and exposed to 1 atm of carbon monoxide (CO). The solution quickly changed from blue to red. After stirring for 5 min, the solution was concentrated to a volume of 10 mL and cooled to -20 °C. Dark red crystals formed (0.67 g, 59% yield). Mp: 125–127 °C. ¹H NMR (C₆D₆, 21 °C): δ 1.17 (s, 36 H, C(CH₃)₃), 4.83 (d, 4H, ⁴J_{CH} = 2 Hz, ring-CH), 5.13 ppm (t, 2H, ⁴J_{CH} = 2 Hz, ring-CH). IR (Nujol mull; CsI windows, cm⁻¹): 1960s, 1880s, 1783m, 1308w, 1258s, 1206m, 1172m, 1055s, 950w, 935w, 922w, 899w, 855w, 830s, 815m, 777s, 766m, 745w, 730w, 705w, 680w, 660w, 565w, 500w, 455w, 400m, 360w, 320w. Anal. Calcd for C₂₈H₄₂O₂Ti: C, 73.35; H, 9.23. Found: C, 73.32; H, 9.41. The EI mass spectrum showed a parent ion at *m/e* = 458 amu. The parent ion isotopic cluster was simulated (calcd %, obsvd %): 456 (10, 8), 457 (13, 12), 458 (100, 100), 459 (38, 36), 460 (15, 12), 461 (3, 0).

Cp₂Ti(PhCCPh). Freshly sublimed diphenylacetylene (0.84 g, 4.7 mmol) and Cp₂Ti (1.0 g, 2.34 mmol) were combined in a Schlenk flask, and hexane was added (50 mL). The mixture produced a dark red solution as it dissolved. Red crystals began to nucleate before all of the diphenylacetylene had dissolved. The solution was cooled to -20 °C, and red-orange crystals were isolated (1.07 g, 75% yield). Mp: 169–170 °C. ¹H NMR (C₆D₆, 21 °C): δ 1.12 (s, 36 H, C(CH₃)₃), 5.51 (d, 4H, ⁴J_{CH} = 2.7 Hz, ring-CH), 7.99 (t, 2H, ⁴J_{CH} = 2.5 Hz, ring-CH), 6.89–7.11 (C₆H₅ resonances, overlapping, 10H). ¹³C NMR (C₆D₆, 21 °C): δ 202.4 (PhCCPh), 144.8 (C₆H₅), 143.5 (ring-CCMe₃), 128.5 (C₆H₅), 127.7 (C₆H₅), 125.6 (C₆H₅), 113.3 (ring-CH), 109.2 (ring-CH), 34.4 (CMe₃), 31.5 (CMe₃). IR (Nujol mull; CsI windows, cm⁻¹): 1642s, 1587s, 1300w, 1250s, 1195w, 1167m, 1065m, 1022m, 975w, 925w, 886w, 839s, 810w, 802w, 791s, 676w, 670s, 709w, 695s, 680w, 675w, 665w, 658w, 605w, 551w, 435m, 399m, 355m, 328m. Anal. Calcd for C₄₀H₅₂Ti: C, 82.73; H, 9.02. Found: C, 82.91; H, 9.14.

Cp₂Ti(C₂H₄). Cp₂Ti (5.8 g, 13 mmol) was dissolved in hexane (50 mL) and exposed to 1 atm of ethylene. The solution changed color from blue to yellow in <5 min. The solution was filtered and concentrated to a volume of 25 mL and cooled to -20 °C. Yellow-green needles formed (2.2 g, 36% yield). Mp: 122–123 °C (dec). ¹H NMR (C₆D₆, 21 °C): δ 1.06 ((s), 36 H, C(CH₃)₃), 2.94 ((s), 4H, C₂H₄), 4.34 (d, 4H, ³J_{CH} = 2.4 Hz, ring-CH), 9.26 (t, 2H,

$^3J_{\text{CH}} = 2.4$ Hz, ring-CH). ^{13}C NMR (C_6D_6 , 21 °C): δ 142.9 (ring- CCMe_3), 119.1 (ring-CH), 108.6 (ring-CH), 97.8 (CH_2CH_2), 34.3 ppm (CMe_3), 32.0 (CMe_3). IR (Nujol mull; CsI windows, cm^{-1}): 1289(m), 1249(s), 1231(m), 1198(m), 1180(w), 1164(m), 1098(s), 1020(m), 944(w), 933(m), 929(m), 918(w), 863(w), 850(s), 817(w), 800(s), 788(s), 725(w), 678(w), 659(s), 610(w), 488(s), 435(m), 384(m), 308(w). Anal. Calcd for $\text{C}_{28}\text{H}_{46}\text{Ti}$: C, 78.11; H, 10.77. Found: C, 77.84; H, 10.87. The EI mass spectrum showed $[\text{M} - (\text{C}_2\text{H}_4)]^+$ as parent ion.

$\text{Cp}'_2\text{TiH}_2$. $\text{Cp}'_2\text{Ti}$ (4.28 g, 10.6 mmol) was dissolved in hexane (50 mL) and exposed to 1 atm of hydrogen. The blue titanocene solution turned dark red. While under the hydrogen atmosphere, the solution was cooled slowly to -80 °C. Dark red crystals were isolated, which were stable with respect to hydrogen loss under vacuum. Mp: 152–154 °C (dec). ^1H NMR (C_7D_8 , -54 °C): δ 1.13 (s, 36 H, $\text{C}(\text{CH}_3)_3$), 2.62 (2H, Ti-H), 5.10 (d, 4H, $^4J_{\text{CH}} = 3$ Hz, ring-CH), 8.01 (t, 2H, $^4J_{\text{CH}} = 3$ Hz, ring-CH). IR (Nujol mull; CsI windows, cm^{-1}): 1640br s, 1295w, 1250s, 1231w, 1202m, 1166m, 1050m, 1024w, 925m, 847m, 821m, 806s, 762m, 722w, 683m, 665m, 464m, 398m. Anal. Calcd for $\text{C}_{26}\text{H}_{44}\text{Ti}$: C, 77.2; H, 10.96. Found: C, 77.28; H, 11.23.

$\text{Cp}'_4\text{Ti}_2(\mu\text{-O})_2$. A 0.45 g (1.05 mmol) portion of $\text{Cp}'_2\text{Ti}(\text{C}_2\text{H}_4)$ was dissolved in ca. 100 mL of pentane, and the solution was exposed to 1 atm of N_2O . The color of the $\text{Cp}'_2\text{Ti}(\text{C}_2\text{H}_4)$ solution changed immediately from yellow-green to bright red, and a red-brown microcrystalline precipitate formed. The solvent was removed under vacuum, and the red-brown powder was extracted into 60 mL of hot toluene and allowed to cool to room temperature and then to -20 °C, yielding the product as red microcrystals (0.4 g, 0.51 mmol, 97%). $\text{Cp}'_4\text{Ti}_2(\mu\text{-O})_2$ was nearly insoluble in pentane and only moderately soluble in toluene and did not react with DMAP or $\text{Cp}'_2\text{Ti}(\text{C}_2\text{H}_4)$. Mp: 228–229 °C (dec). ^1H NMR (C_6D_6 , 21 °C): δ 1.36 (s, 18H, $\text{C}(\text{CH}_3)_3$), 1.45 (s, 18H, $\text{C}(\text{CH}_3)_3$), 5.78 (d, 2H, $^4J_{\text{CH}} = 1.3$ Hz, ring-CH), 6.04 (d, 2H, $^4J_{\text{CH}} = 2.7$ Hz, ring-CH), 6.33 (t, 1H, $^4J_{\text{CH}} = 1.3$ Hz, ring-CH), 6.53 (t, 1H, $^4J_{\text{CH}} = 2.7$ Hz, ring-CH). IR (Nujol mull; CsI windows, cm^{-1}): 3080(w), 2654(sh), 1255(m), 1205(w), 1182(w), 1148(w), 1040(w), 1023(w),

930(m), 858(s), 828(s), 810(m), 800(s), 729(br.s), 680(m), 620(br.s), 468(m), 428(sh), 402(m), 359(m), 295(w), 259(m). Anal. Calcd for $\text{C}_{52}\text{H}_{84}\text{O}_2\text{Ti}$: C, 74.61; H, 10.12. Found: C, 74.61; H, 10.01. The EI mass spectrum showed a parent ion at $m/e = 837$ amu. The parent ion isotopic cluster was simulated (calcd %, obsvd %): 834 (2, 2), 835 (10, 9), 836 (29, 28), 837 (100, 100), 838 (69, 70), 839 (37, 37), 840 (14, 15), 841 (4, 3). However, the EI-MS also shows a higher mass fragment due to $[\text{Cp}_4\text{Ti}_4\text{O}_4]^+$.

Acknowledgment. This work was supported by the Director, Office of Science, Office of Basic Energy Sciences, Material Sciences and Engineering Division of the U.S. Department of Energy under Contract DE-AC02-05CH11231. We thank Dr. Fred Hollander (at CHEXRAY, the U.C. Berkeley X-ray diffraction facility) for assistance with the crystallography, the German Academic Exchange Service (DAAD) for a fellowship (M.D.W.), and Wayne W. Lukens for discussions and assistance with the EPR studies.

Supporting Information Available: Crystallographic data, labeling diagrams, tables giving atomic positions, anisotropic thermal parameters, bond distances, bond angles, torsion angles, least-squares planes for each structure, solid state magnetism data (χ_{m}^{-1} vs T and μ_{eff} vs T plots) for $\text{Cp}'_2\text{TiX}$ ($X = \text{Cl}, \text{Me}, \text{OH}, \text{H}$) and $\text{Cp}''_2\text{TiCl}$, UV-vis spectra for $\text{Cp}''_2\text{TiCl}$ and $(\text{Cp}''_2\text{Ti})_2(\text{N}_2)$, and Hildebrand–Benesi plot for $\text{Cp}'_2\text{TiH}_2$. This material is available free of charge via the Internet at <http://pubs.acs.org>. Structure factor tables are available from the authors. Crystallographic data were also deposited with Cambridge Crystallographic Data Centre. Copies of the data (CCDC 662583–662585) can be obtained free of charge via http://www.ccdc.cam.ac.uk/data_request/cif, by e-mailing data_request@ccdc.cam.ac.uk, or by contacting The Cambridge Crystallographic Data Centre, 12 Union Road, Cambridge CB 1EZ, UK; fax +44 1223 336033.

OM7012315